

AD-A156 304

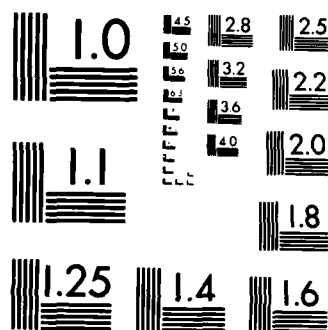
THE INFLUENCE OF HELICOPTER TAIL SHAPE ON DRAG: AN
AERODYNAMIC STUDY USING A LOW SPEED WIND TUNNEL(U)
NAVAL POSTGRADUATE SCHOOL MONTEREY CA C L SARGENT
MAR 85 F/G 20

1/1

UNCLASSIFIED

F/G 20/4

NL



MICROCOPY RESOLUTION TEST CHART
NATIONAL BUREAU OF STANDARDS-1963-A

AD-A156 304

2

NAVAL POSTGRADUATE SCHOOL

Monterey, California



DTIC
ELECTE
JUL 3 1985
S B

THESIS

DTIC FILE COPY

THE INFLUENCE OF HELICOPTER TAIL SHAPE ON DRAG
AN AERODYNAMIC STUDY
USING A LOW SPEED WIND TUNNEL

by

Christopher L. Sargent

March 1985

Thesis Advisor: Donald M. Layton

Approved for public release; Distribution is unlimited

85 6 / 25 038

DISCLAIMER NOTICE

**THIS DOCUMENT IS BEST QUALITY
PRACTICABLE. THE COPY FURNISHED
TO DTIC CONTAINED A SIGNIFICANT
NUMBER OF PAGES WHICH DO NOT
REPRODUCE LEGIBLY.**

REPORT DOCUMENTATION PAGE		READ INSTRUCTIONS BEFORE COMPLETING FORM
1. REPORT NUMBER	2. GOVT ACCESSION NO. AD-A156	3. RECIPIENT'S CATALOG NUMBER 304
4. TITLE (and Subtitle) The Influence of Helicopter Tail Shape on Drag An Aerodynamic Study Using a Low Speed Wind Tunnel		5. TYPE OF REPORT & PERIOD COVERED Master's Thesis March 1985
		6. PERFORMING ORG. REPORT NUMBER
7. AUTHOR(s) Christopher L. Sargent		8. CONTRACT OR GRANT NUMBER(s)
9. PERFORMING ORGANIZATION NAME AND ADDRESS Naval Postgraduate School Monterey, California 93943		10. PROGRAM ELEMENT, PROJECT, TASK AREA & WORK UNIT NUMBERS
11. CONTROLLING OFFICE NAME AND ADDRESS Naval Postgraduate School Monterey, California 93943		12. REPORT DATE March 1985
		13. NUMBER OF PAGES 90
14. MONITORING AGENCY NAME & ADDRESS (if different from Controlling Office)		15. SECURITY CLASS. (of this report)
		15a. DECLASSIFICATION/DOWNGRADING SCHEDULE
16. DISTRIBUTION STATEMENT (of this Report) Approved for public release, distribution unlimited		
17. DISTRIBUTION STATEMENT (of the abstract entered in Block 20, if different from Report)		
18. SUPPLEMENTARY NOTES		
19. KEY WORDS (Continue on reverse side if necessary and identify by block number) Helicopter, Drag, Wind Tunnel, Drag of helicopter tail shape		
20. ABSTRACT (Continue on reverse side if necessary and identify by block number) This thesis examines the effect of helicopter tail shape on drag using a low speed wind tunnel at the Naval Postgraduate School. A modification to the Aeronautical Engineering Department's 3.5' x 5' wind tunnel was made		

to update facilities and allow this work. Major R. Scott Mair worked simultaneously to study the effect of nose shape on drag, a result of the 2-man requirement for wind tunnel work. The existing external balance was replaced with an internal balance and a variable angle-of-attack support system was constructed as well. Quantitative data was collected with this balance, and qualitative information was obtained by tufting the models and visualizing the airflow. The equipment built was adequate with the exception of one component of the balance, which will require a new balance to be built. This single deficiency was significant enough to invalidate the output of the balance and as a result any quantitative discussion of how a helicopter's tail shape affects drag. Without this data the explanation of drag using flow visualization is also not practical.

Approved for Release	✓
by	
on	
Authority	
Remarks	
A-1	

Approved for public release; distribution is unlimited.

The Influence of Helicopter Tail Shape on Drag
An Aerodynamic Study
Using a Low Speed Wind Tunnel

by

Christopher L. Sargent
Captain, United States Army
B.S., United States Military Academy, 1974

Submitted in partial fulfillment of the
requirements for the degree of

MASTER OF SCIENCE IN AERONAUTICAL ENGINEERING

from the

NAVAL POSTGRADUATE SCHOOL
March 1985

Author:

Christopher L. Sargent

Christopher L. Sargent

Approved by:

Donald M. Layton

Donald M. Layton, Thesis Advisor

Max F. Platzer

Max F. Platzer, Chairman,
Department of Aeronautics

John N. Dyer

John N. Dyer,
Dean of Science and Engineering

ABSTRACT

This thesis examines the effect of helicopter tail shape on drag using a low speed wind tunnel at the Naval Postgraduate School. A modification to the Aeronautical Engineering Departments' 3.5'x 5' wind tunnel was made to update the facilities and allow this work. Major R. Scott Mair worked simultaneously to study the effect of nose shape on drag, a result of the 2-man requirement for wind tunnel work. The existing external balance was replaced with an internal balance and a variable angle-of-attack support system was constructed as well. Quantitative data was collected with this balance, and qualitative information was obtained by tufting the models and visualizing the airflow. The equipment built was adequate with the exception of one component of the balance, which will require a new balance to be built. This single deficiency was significant enough to invalidate the output of the balance and as a result any quantitative discussion of how a helicopter's tail shape affects drag. Without this data the explanation of drag, using flow visualization alone is also not practical.

TABLE OF CONTENTS

I.	INTRODUCTION	11
	A. COORDINATION OF EFFORT	11
	B. BACKGROUND	11
	C. QUALITATIVE DATA	12
	D. QUANTITATIVE DATA	13
	E. GOALS	13
II.	APPROACH TO THE PROBLEM	14
	A. MODEL DESIGN	14
	1. Concept	14
	2. Shapes	15
	3. Construction	15
	B. WIND TUNNEL MODIFICATION	18
	1. Tunnel Design	18
	2. Test Section Environment	18
	C. BALANCE DESIGN	21
	1. Concept	21
	2. Calibration	24
	3. Instrumentation	24
III.	SOLUTION TO THE PROBLEM	29
	A. DATA COLLECTION	29
	B. DATA REDUCTION	29
	C. GRAPHICAL ANALYSIS	30
	D. FLOW VISUALIZATION	30
IV.	RESULTS	32
	A. QUANTITATIVE	32
	B. QUALITATIVE	33

V.	CONCLUSIONS AND RECOMMENDATIONS	35
A.	CONCLUSIONS	35
B.	RECOMMENDATIONS	35
	APPENDIX A: TABLES, FIGURES, AND PROGRAMS	41
	APPENDIX B: GRAPHICAL RESULTS	76
	APPENDIX C: FLOW VISUALIZATION RESULTS	79
	LIST OF REFERENCES	88
	BIBLIOGRAPHY	89
	INITIAL DISTRIBUTION LIST	90

LIST OF TABLES

1. Balance Calibration Data, Normal Component 57
2. Balance Calibration Data, Axial Component 58

LIST OF FIGURES

2.1	Common Fuselage with Nose and Tail Sections	14
2.2	Attack Nose with High Tail	15
2.3	Attack Nose with Symmetric Tail	15
2.4	Attack Nose with Low Tail	16
2.5	Blunt Nose with High Tail	16
2.6	Blunt Nose with Symmetric Tail	16
2.7	Blunt Nose with Low Tail	17
2.8	Smooth Nose with High Tail	17
2.9	Smooth Nose with Symmetric Tail	17
2.10	Smooth Nose with Low Tail	18
2.11	3.5 x 5 foot Low Speed Wind Tunnel	19
2.12	Preexisting External Balance	20
2.13	Sting Support Mounted in Test Section	21
2.14	Flow Angularity at Model Location	22
2.15	Balance Design with Component Description	23
2.16	Visualization of Balance Interaction	25
2.17	Flow Chart for Data Correction Due to Balance Interaction	26
2.18	Calibration Rig for Axial and Normal Channels	27
2.19	Electrical Instrumentation	27
2.20	Principle of Low-Pass Filter	28
5.1	Proposed 4-Channel Balance Design	37
5.2	Vibration Damping System, 1st Design	38
5.3	Vibration Damping System, 2nd Design	39
A.1	Planview of Blunt Nose	41
A.2	Planview of Attack Nose	42
A.3	Planview of Smooth Nose	43
A.4	Planview of Symmetric Tail	44

A.5	Planview of High/Low Tail	45
A.6	Planview of Common Fuselage	46
A.7	Planview of Sting Support System	47
A.8	Raw Data Files	48
A.9	FORTTRAN Program for Data Conversion	59
A.10	Data Collection Checklist	64
A.11	Data Output Files	66
A.12	Layout for Mini-tufting Photography	75
B.1	Cd Versus AOA	76
B.2	Cd Versus Cl	77
B.3	Cd Versus Cl Squared	78
C.1	Attack Nose/ High Tail	79
C.2	Attack Nose/ Symmetric Tail	80
C.3	Attack Nose/ Low Tail	81
C.4	Blunt Nose/ High Tail	82
C.5	Blunt Nose/ Symmetric Tail	83
C.6	Blunt Nose/ Low Tail	84
C.7	Smooth Nose/ High Tail	85
C.8	Smooth Nose/ Symmetric Tail	86
C.9	Smooth Nose/ Low Tail	87

ACKNOWLEDGEMENTS

To Ron Ramaker for his artistic effort in crafting a superb model and Bob Besel for his technical advice and time taken in procuring all the required hardware. To Glenn Middleton for his precise machine work and patient understanding in the process, and Ted Dunton for his sage advice so well needed when seen in retrospect. Their advice, experience, and humor was invaluable and made this project truly enjoyable.

I. INTRODUCTION

A. COORDINATION OF EFFORT

Successful and safe operation of a wind tunnel project requires at least two people in full-time involvement, either the investigator and an assistant/technician, or co-investigators. Inasmuch as this was an unfunded project, there was no full-time technician available and, as a result, a coordinated effort was conducted with the thesis project of another Master of Science in Aeronautical Engineering student, Major Mair [Ref. 1].

Even though a deliberate effort was made to separate the majority of functions in the two projects, e.g., design of the test and calibration equipment - Mair and design of the models, sting support, and balance - Sargent, when two people work closely together, much of the output is the result of proposals and counter-proposals, and their contributions are difficult to distinguish.

The differences, however, in the scope and outcomes of the experiment dictate that the results of these efforts, no matter how great the coordination, be presented as two separate theses.

B. BACKGROUND

Although exhaustive analyses of helicopter drag have been made, aerodynamic modelling has not been an area of concentration at the Naval Postgraduate School. However, determination of both qualitative and quantitative fuselage drag parameters is an essential part of the education process, and, in particular, is a valuable adjunct to helicopter design courses.

Previously, quantitative data at the Naval Postgraduate School low-speed wind tunnels were obtained with 'external' balance systems placed outside the tunnel and measurements were made through struts passing through the tunnel floor to the model. Not only was this

technique dated, none of the balance systems worked properly and in order to make precise measurements it was necessary to borrow a balance from the NASA Ames Research Laboratory. This not only inhibited continuing work in this area, but in addition, the risk of loss or damage to the NASA system was intolerable.

It was decided that an 'internal' balance that could be located inside the model would not only provide the information required for the project at hand, but, if designed with a universal mount, such a balance could be used for other fixed and rotary wing models. And, if such a balance could be constructed at low cost (this being an unfunded project), it would provide the Department of Aeronautics with an in-house capability that did not currently exist.

Such a balance was designed by the author, with the aid of a Russian design [Ref. 2: pp. 412-414], constructed by the Department of Aeronautics, and installed in the 3.5' x 5' Aerolab wind tunnel in Building 234 at the Naval Postgraduate School.

C. QUALITATIVE DATA

Although a properly designed wind tunnel balance can provide quantitative information as to lift, drag and moments, such information may not be enough to fully explain what is causing these forces and moments. A flow visualization technique that would permit a qualitative examination of the potential field about the model would be a welcome addition to a modelling process, but if this visualization process did not produce interference forces on the model, such a qualitative examination would be extremely worthwhile.

Such an advanced technique was available through the use of 'Mini-tufting' [Ref. 3]. The nearly microscopic strands of fluorescent monofilament line are permanently mounted on the surface of the model and do not interfere with force measurements.

D. QUANTITATIVE DATA

A variable angle-of-attack sting system was designed that would permit pitch rotation about both the center of the balance and the center of the model. This system was mounted in the wind tunnel with provisions for external control of the angle-of-attack. The balance and the model were supported by this sting system.

E. GOALS

The primary purpose of this project was to produce a helicopter wind tunnel model, balance system and instrumentation that could provide experimental data to be used by students in the helicopter design classes for the development of realistic Equivalent Flat Plate area information for several types of helicopters.

Secondary purposes established during the conduct of the project included the development of a two-axis internal wind tunnel balance with a universal mount and the addition of flow visualization to the quantitative determinations.

II. APPROACH TO THE PROBLEM

A. MODEL DESIGN

1. Concept

To provide a selection of fuselage shapes for comparison, three noses and three tails were chosen representing existing as well as more advanced technologies in helicopter design. The author prepared planviews (Figures A.1-A.5) from which the nose and tail sections were made. To make comparisons of lift and drag between these nine model combinations, and yet not introduce too many variables, the concept of a fuselage, common to each combination was also designed by the author and built (Figure A.6). To this each nose and tail could be mounted, each with the same cross-sectional shape and mounting system (Figure 2.1)



Figure 2.1 Common Fuselage with Nose and Tail Sections

2. Shapes

By first considering one nose, and then evaluating the effect of each of the three tails, a comparison of tail shapes could be made. This was done for each of the noses for a total of nine model combinations (Figures 2.2-2.10).

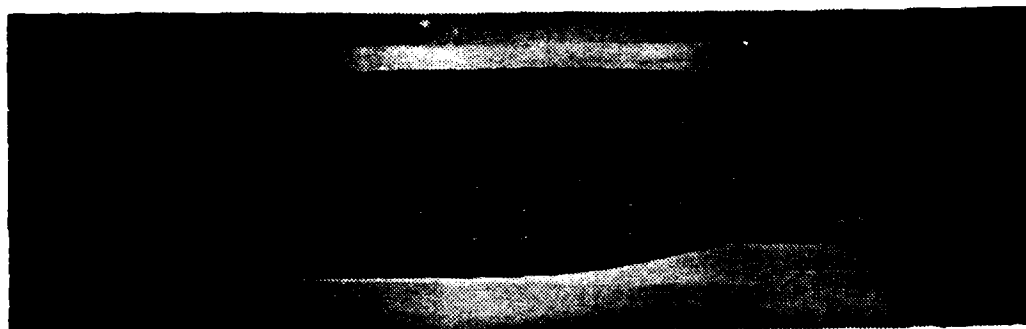


Figure 2.2 Attack Nose with High Tail

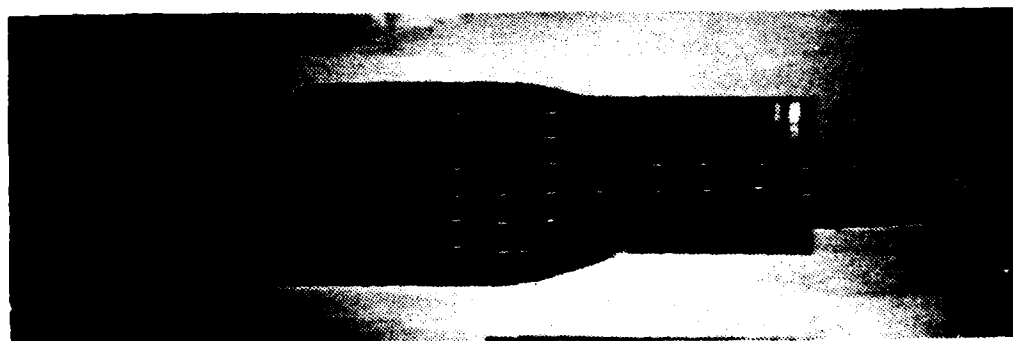


Figure 2.3 Attack Nose with Symmetric Tail

3. Construction

All parts of the model were constructed of aluminium and wood with screws and bolts used as fasteners. The center fuselage is a rigid box of metal with metal end plates and a filling of wood to form

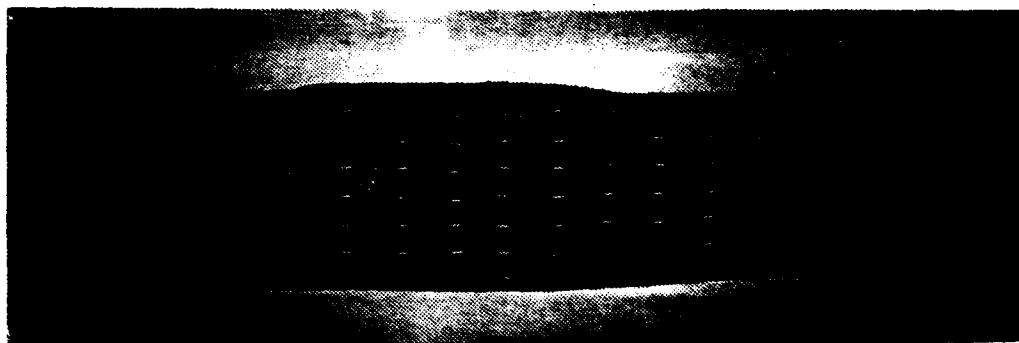


Figure 2.4 Attack Nose with Low Tail

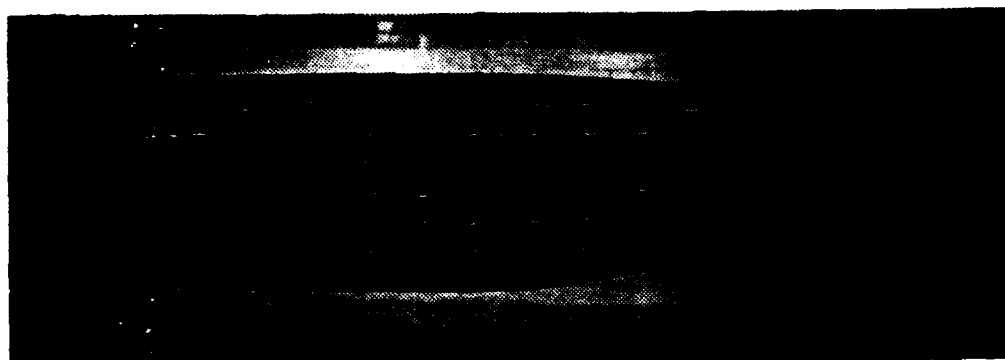


Figure 2.5 Blunt Nose with High Tail

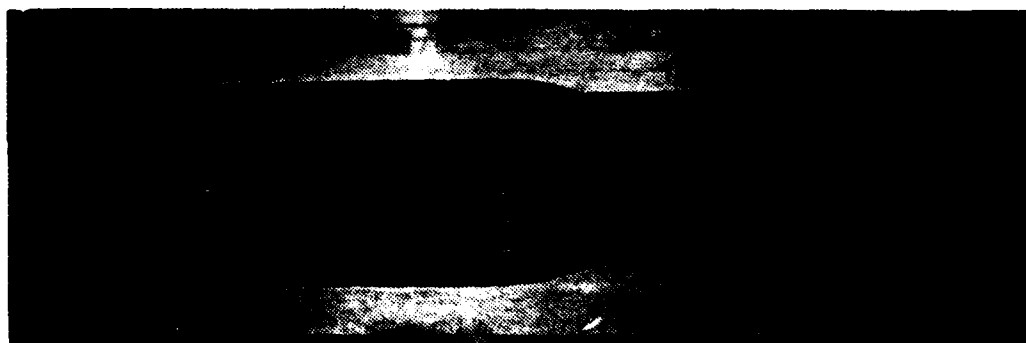


Figure 2.6 Blunt Nose with Symmetric Tail

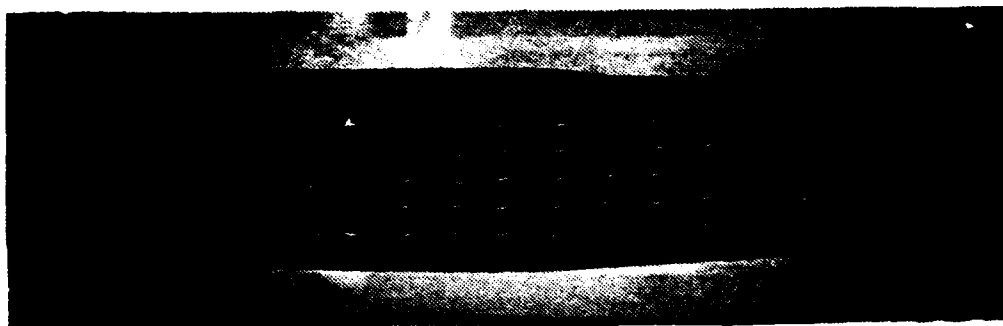


Figure 2.7 Blunt Nose with Low Tail

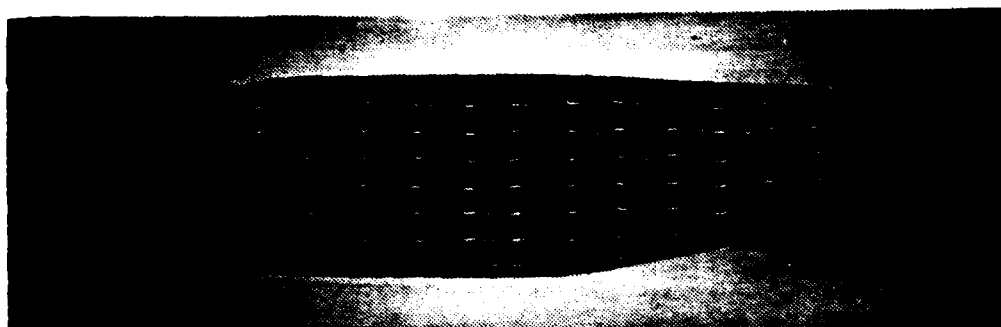


Figure 2.8 Smooth Nose with High Tail

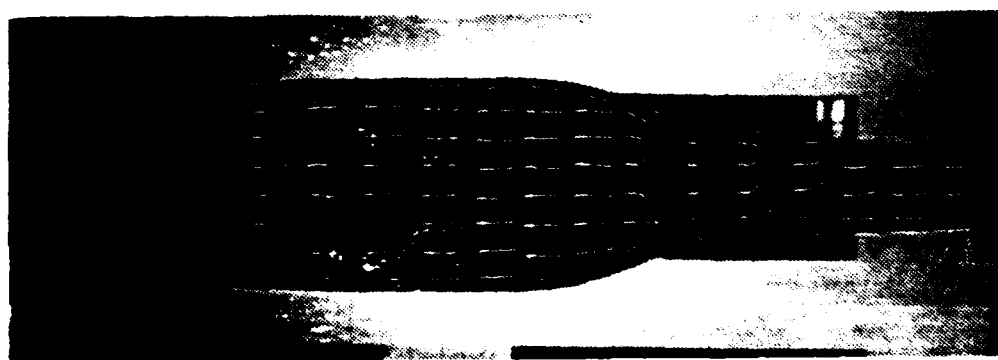


Figure 2.9 Smooth Nose with Symmetric Tail

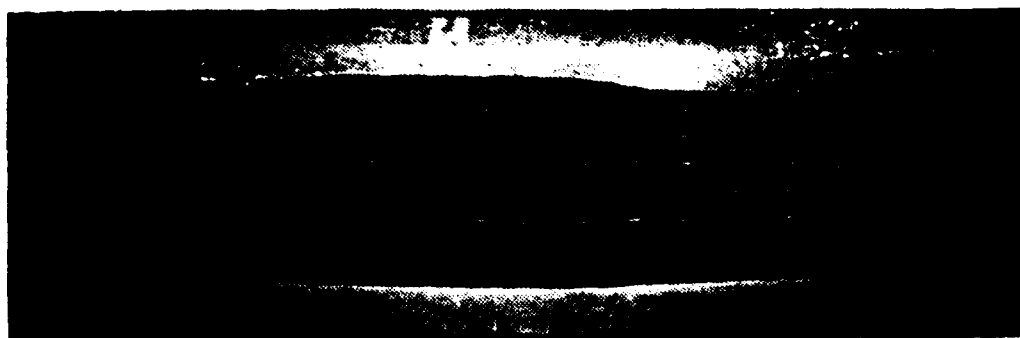


Figure 2.10 Smooth Nose with Low Tail

the skin. Three bars of metal run the length of each side of the common fuselage to form a screw-in mounting for landing gear, wing stores supports, etc., for future expansion. The noses and tails are wood, for the most part, and have metal end plates for a uniform joining surface.

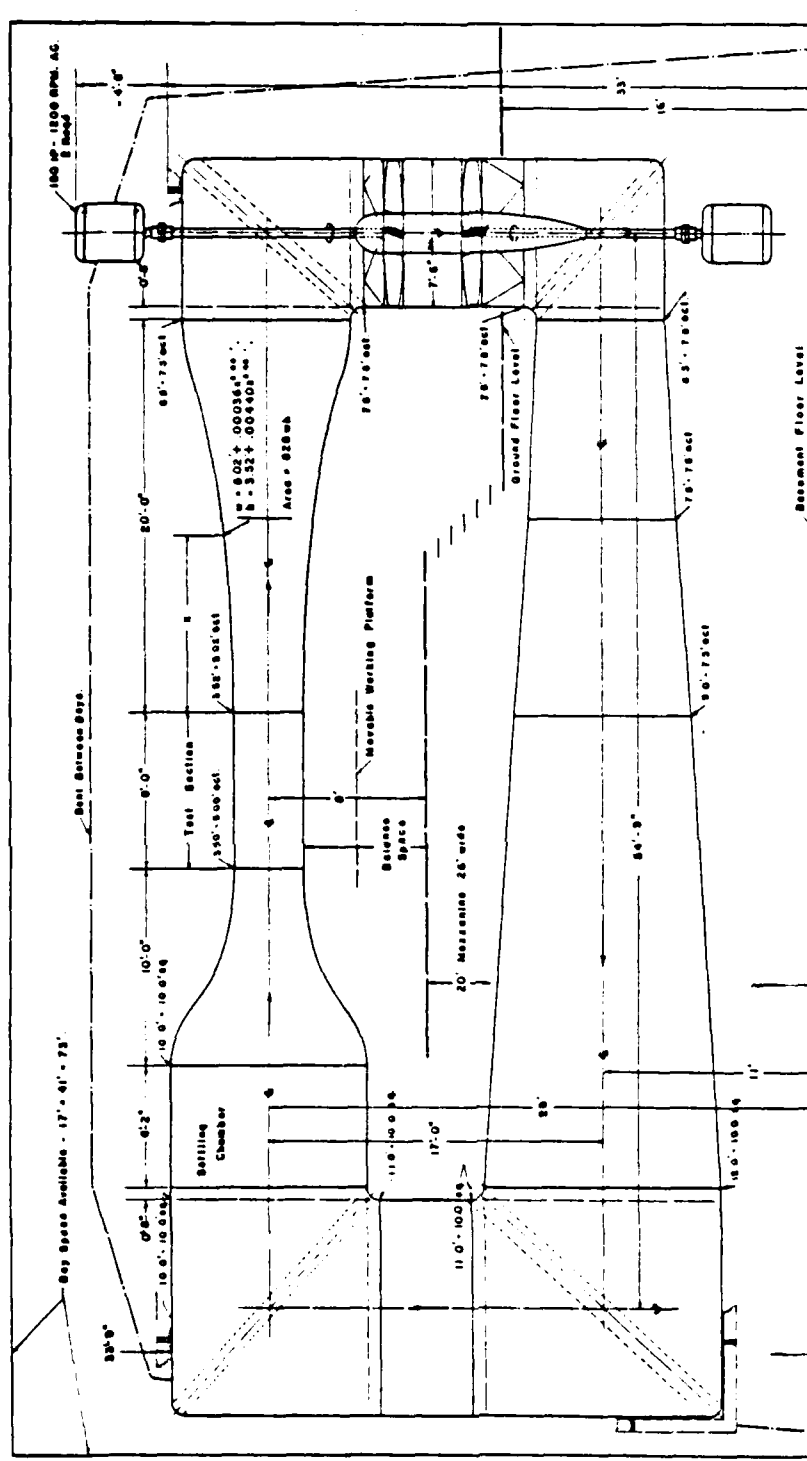
B. WIND TUNNEL MODIFICATION

1. Tunnel Design

Figure 2.11 shows the wind tunnel used in the Aeronautical Engineering Department. The external balance used previously (Figure 2.12) was dismantled and the floor of the test section replaced for the sting support system (Figure 2.13). This was designed by the author, a planview of which is included in Figure A.7 This support to which the balance is mounted, fixes the center of the balance in space (and therefore the pitching axis of the model) and allows for an angle of attack change of $+10$ to -12 degrees.

2. Test Section Environment

Tests were made for cross-sectional wind tunnel velocity and angularity at the location of the model in the tunnel. A cross-sectional mapping of velocity produced a very uniform distribution of velocity.



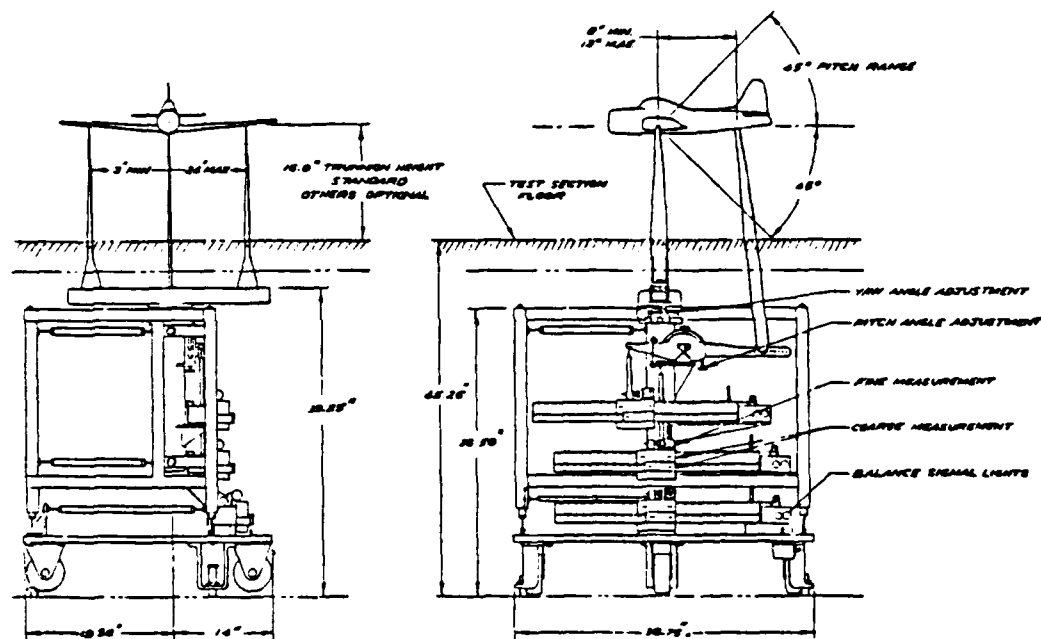
3.5 ft. x 5.0 ft. - 200 knot ACADEMIC WIND TUNNEL.

U. S. NAVAL POSTGRADUATE SCHOOL.

MONTEREY, CALIFORNIA

Overall Dimensions 118'-0" x 38'-0" x 63'-0"

Figure 2.11 3.5 x 5 foot Low Speed Wind Tunnel



AEROLAB 3 COMPONENT BEAM BALANCE

Figure 2.12 Preexisting External Balance

This distribution was made by running a pitot static probe across the tunnel from each of the eight tunnel walls, creating a 'spider web', that effectively mapped the cross-sectional area. Measuring the angularity, or twist, of the flow was done by attaching a yaw probe to the traversing system used for measuring velocity. This gave a map (Figure 2.14) of the angularity as viewed from upwind looking into the test section for dynamic pressures of 20, 30, and 40 psf. The tunnel initially had two counter-rotating sets of blades, eliminating most of the twist in the flow, but one set had been previously damaged and could not be repaired. This produced a flow with more angularity than desired. Twist was severe at the tunnel walls, but was moderate in the vicinity of the model location. Because only trends were being compared, and each model was affected similarly, the effects of angularity were not corrected. A further reason for neglecting the influence of this flow was that planar surfaces such as wings or tails that would have been noticeably affected were not used.

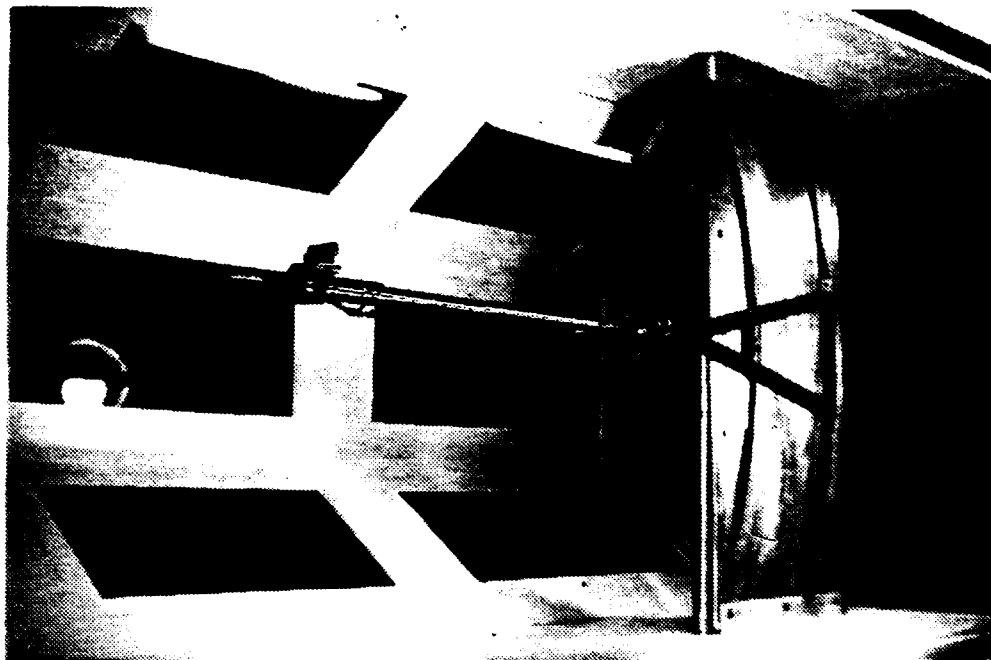
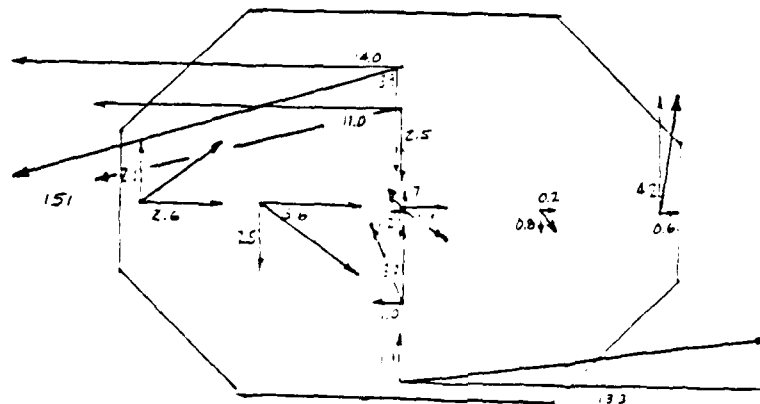
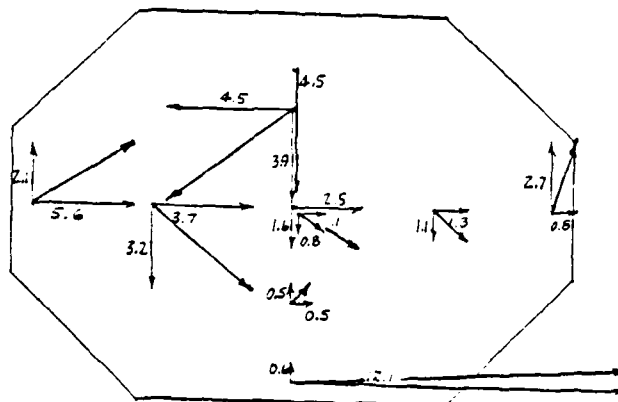
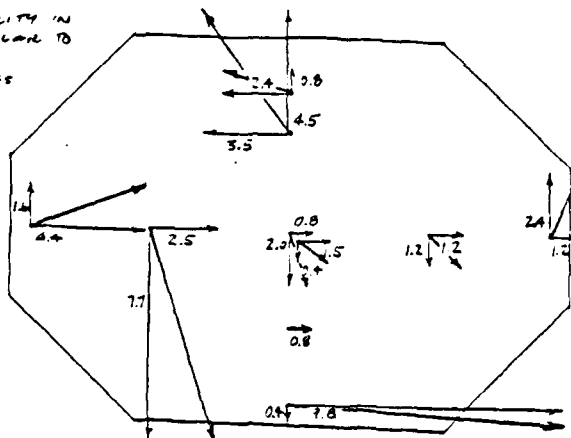


Figure 2.13 Sting Support Mounted in Test Section

C. BALANCE DESIGN

1. Concept

Initially a balance was desired that would measure all forces and moments that the model could experience. The difficulties in fabricating one with this capability, on the other hand, were numerous and would have required more time than was available. The design for a three-component balance was taken from one designed for use with small caliber projectiles, but modified, in that a 25 pound model had to be supported [Ref. 2: pp. 412-414]. This design gave lift, drag, and pitching moment, of which only the normal and axial(for lift and drag) channels were used. Figure 2.15 depicts the design of the balance as well as how each component works. The normal and axial components consist of elastic parallelograms that distort slightly, producing localized tension and compression in the webs.

TUNNEL ANGLE

22

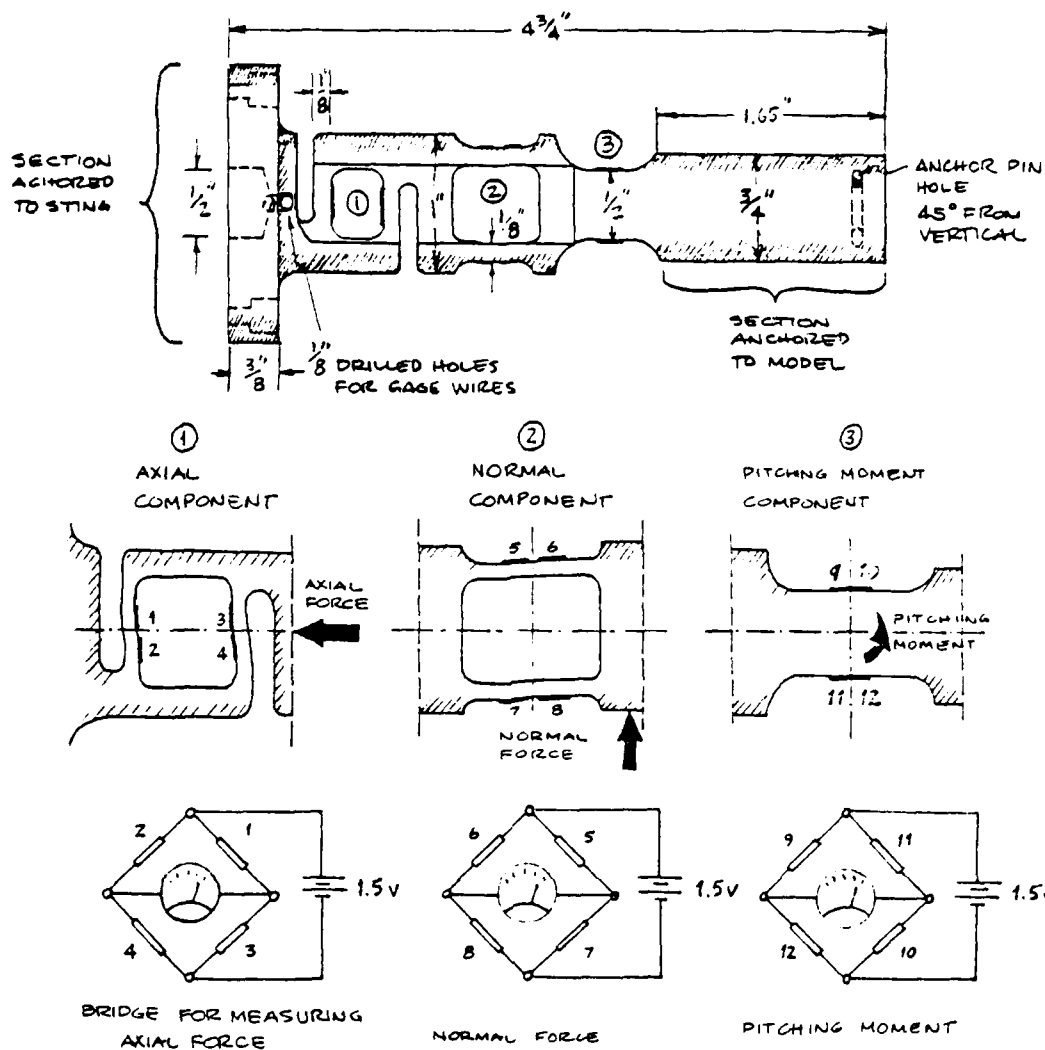


Figure 2.15 Balance Design with Component Description

Strain gages applied to these locations measured the elastic deformation that resulted, and hence the amount of force applied [Ref. 4: pp. 364-370]. The pitching moment component was of cantilever design with a positive pitching moment producing compression in the top surface and tension in the bottom.

Each component had four gages wired into a Wheatstone bridge which could be balanced (zeroed) once the weight of each model was applied [Ref. 4: pp. 110-111].

2. Calibration

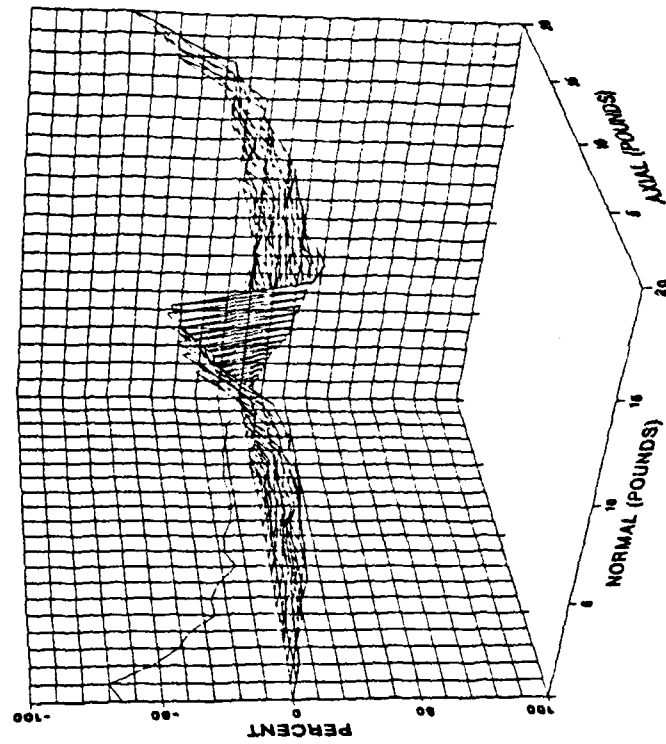
The balance was calibrated to identify any interaction between normal and axial loading. A calibration rig consisted of the common fuselage and balance mounted on the sting at zero angle of attack(AOA). Using pinned fittings shown in Figure 2.18, the axial and normal components could be loaded independently. The wheatstone bridge for each component was balanced (zeroed) once the rig was in place. Weights from 0-20 pounds were placed on the pans, one pound at a time, producing a 20x20 matrix of 'raw' normal counts and one of axial counts (Figure A.8). Some interaction was present, as seen in Figure 2.16, where the degree of error can be seen as peaks (above expected readings) and valleys (below). A flat surface would indicate no interaction. The interaction surfaces are somewhat deceiving in that small errors at low loading conditions produced relatively large errors (peaks and valleys). A computer program was used to correct the actual data collected for interaction error, reducing its effect considerably (Figure 2.17 depicts the flow chart used).

3. Instrumentation

Figure 2.19 depicts a block diagram of the instrumentation used. The signal from each channel was split, allowing a raw reading and a conditioned reading. It was found that the movement of the model produced enough noise to cause the raw reading to be unreadable during normal operation.

A low pass filter, shown conceptually in Figure 2.20, was used to eliminate all frequencies above .5 hertz [Ref. 4: pp. 129-130]. This value was determined experimentally by plucking the nose of the model to introduce noise and varying the low cutoff frequency. At .5 hertz enough of the higher frequency vibrations had been eliminated to cause the conditioned signal to be readable. Lowering the cutoff frequency any further increased the settling time of the readout to where it became excessive(greater than 10 seconds).

HOW NORMAL LOADING AFFECTS AXIAL COMPONENT



HOW AXIAL LOADING AFFECTS NORMAL COMPONENT

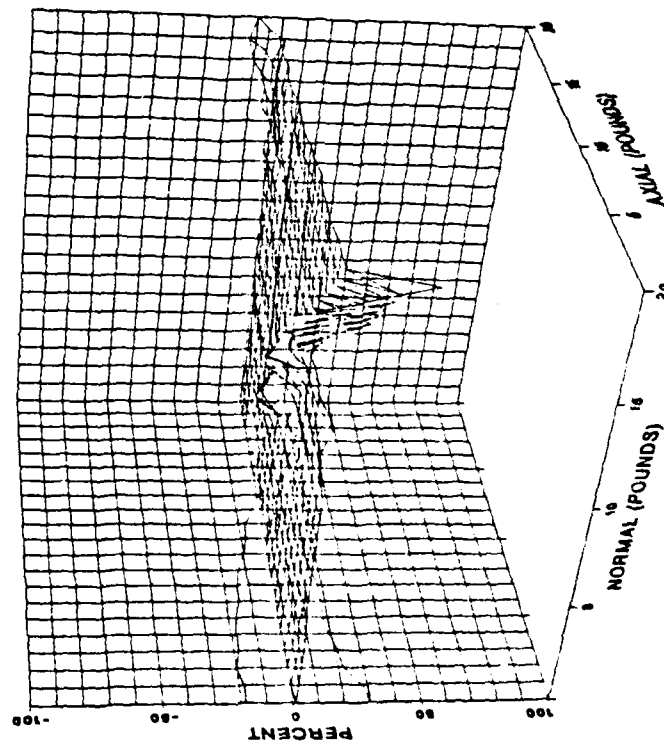


Figure 2.16 Visualization of Balance Interaction

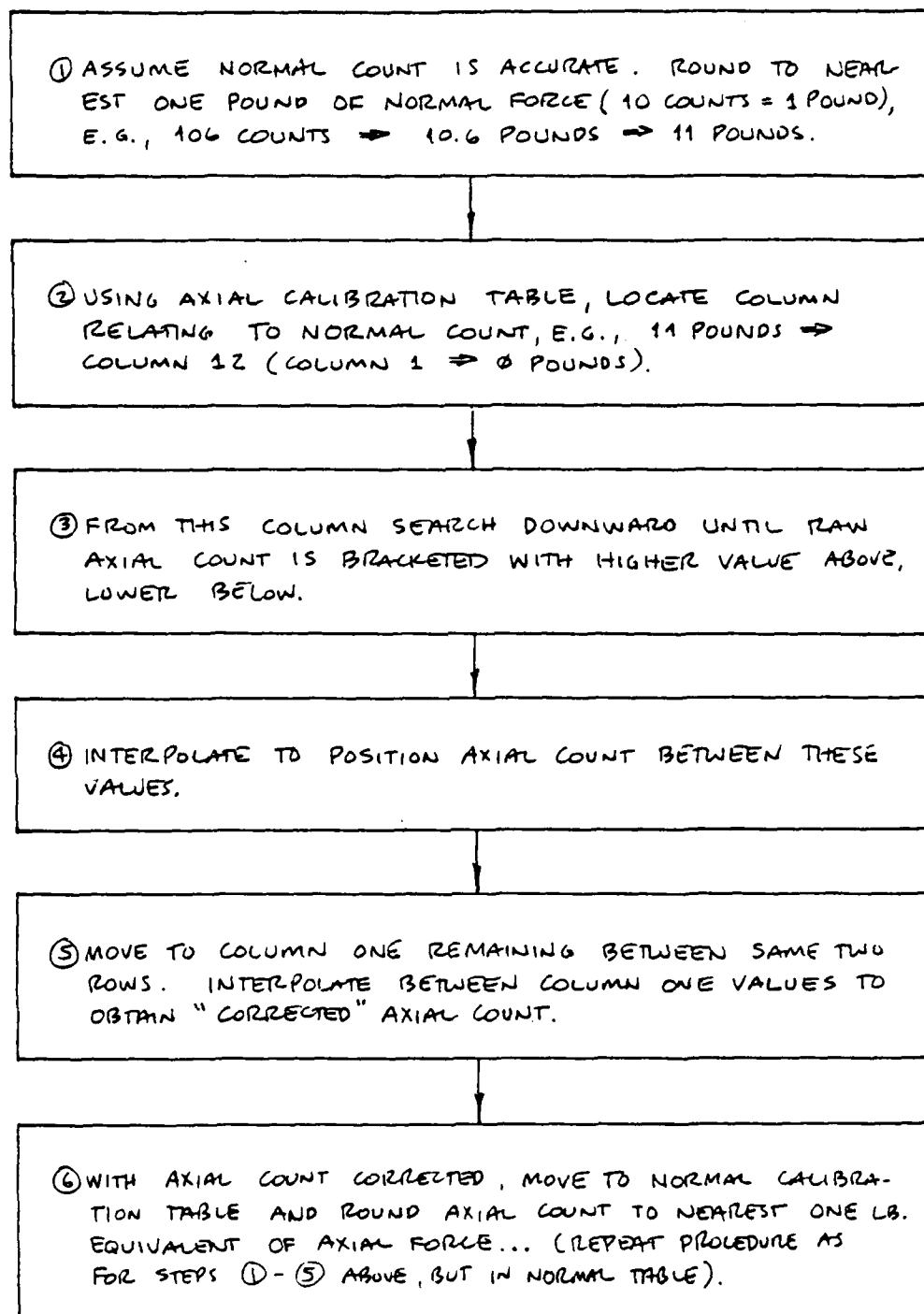


Figure 2.17 Flow Chart for Data Correction Due to Balance Interaction

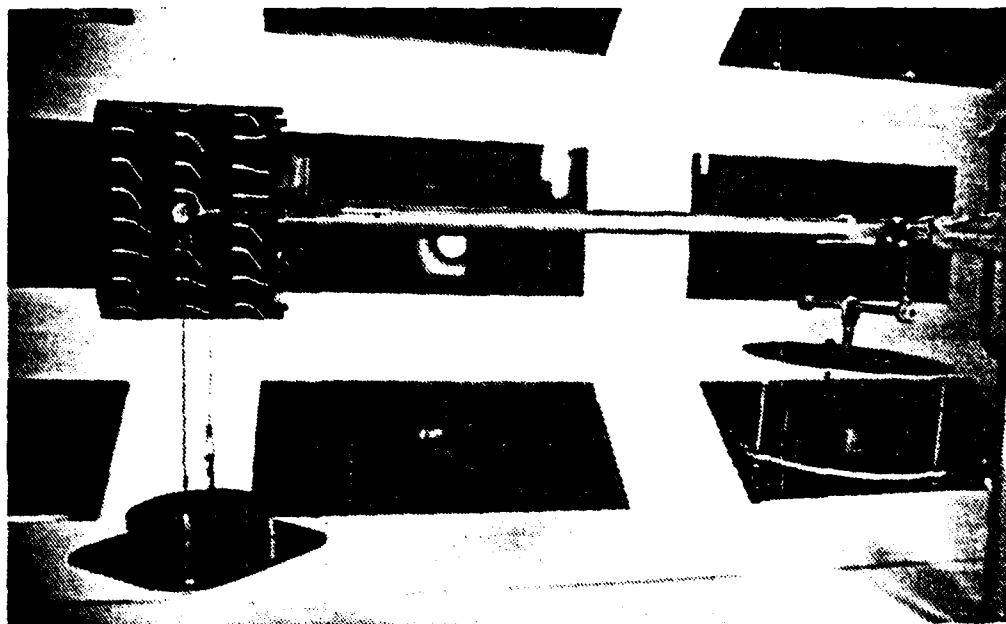


Figure 2.18 Calibration Rig for Axial and Normal Channels

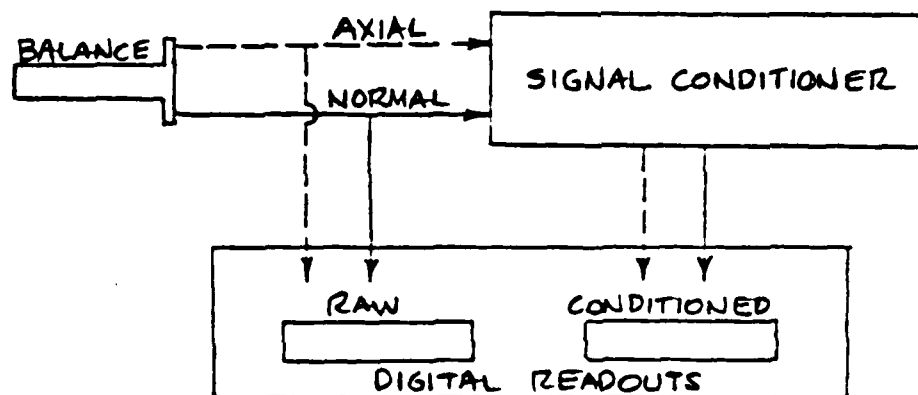


Figure 2.19 Electrical Instrumentation

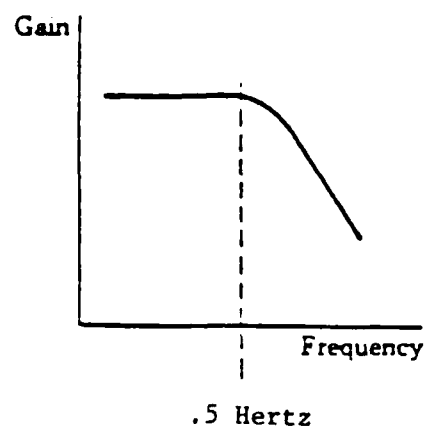


Figure 2.20 Principle of Low-Pass Filter

III. SOLUTION TO THE PROBLEM

A. DATA COLLECTION

To restrict the volume of information to be collected to a reasonable amount, the number of variables was limited. Four tunnel speeds were chosen for Q's of 10, 30, 50, and 70 psf, as were ten angles of attack, from +8 to -10 degrees, in 2 degree increments. Data was collected from digital readouts by hand, requiring 80 readings per model, a manageable number.

To standardize data collection a checklist was used prior to the testing of each model (Figure A.10). The balance and electrical equipment were calibrated before each data run (within 20 minutes) and afterwards with the zeroed readings drifting slightly if this time was exceeded. Figure A.8 contains a listing of the 9 data files, each reading taken in raw counts of normal and axial force (not corrected for balance interaction or the weight of the model).

B. DATA REDUCTION

Circuit boards used to provide an excitation voltage for each of the Wheatstone bridges (one per channel), and to amplify their output, were adequate, but only after many boards had been checked and discarded as faulty. The use of two digital voltmeters as displays, with one per channel, was good in that the decimal point could be varied to match the bridge outputs. The number of significant digits in the output was not initially known, but by varying the amplification for each channel, until noise prevented any further amplification, the decimal point was fixed and noisy digits were truncated. The number of significant digits that were readable (three) eventually became the number of digits in the 'counts' readout (where 10 pounds became 100 counts).

A FORTRAN program was written by Major Mair to convert the raw counts of normal and axial force to pounds of lift and drag(Figure A.9). From this the coefficients of lift and drag, and the equivalent flat plate area were calculated(Figure A.11). To determine these values, the raw counts were first corrected for balance interaction, then the weight of the model(as a function of AOA), was removed. The remaining counts were then converted to counts of lift and drag, used directly to solve for the required coefficients. To add a visual meaning to this data several parameters were plotted against one another.

C. GRAPHICAL ANALYSIS

Plotting all of the available parameters, for each of the given airspeeds, would produce too many curves. The following comparisons were made at Q's of 30 and 70 psf (Figures B.1-B.3).

1. Cd versus AOA
2. Cd versus Cl
3. Cd versus Cl squared

D. FLOW VISUALIZATION

The explanation of what causes lift and drag is not easily explained by numerical or a graphical interpretation. Instead, other techniques are required that augment the quantitative data, and in this situation tufting was used. 'Mini-tufting' the model was the desired method, but a strobe, possibly inadequate for the conditions of photography, prevented an extended trial an error development of the technique [Ref. &mini]. Instead, cotton tufting was used under floodlamp illumination to produce the desired results. Pictures were taken of sideviews of the model for AOA's of +8, 0, and -10 degrees for Q's of 30 and 70. This produced 54 pictures which were augmented with frontal and rear views as deemed necessary to explain the flow (Figures C.1-C.9). The film used was Tri-X by Kodak (ASA 400), pushed to 1200 and developed into contact prints. From these prints, the desired exposures were chosen and developed into useable full size prints and

halftones. The lens used were a 28-80mm macro-zoom for the side views and a Nikon 50mm for the front and rear views. The exposures were taken at 1/30th second and an F-stop of 5.6.

IV. RESULTS

A. QUANTITATIVE

The experimental hardware developed during the course of this thesis produced good results with some adjustments required for further testing. The physical arrangement of the sting support system, balance, and models all worked well and were relatively easy to work with. The support was sufficiently stiff enough to maintain model attitude under all wind tunnel conditions, and the balance, initially considered marginal in strength, was elastic enough to produce good strain gage output without plastic deformation. The electrical instrumentation was adequate in that only two channels, axial and normal required signal conditioning. Had more channels been necessary, conditioning would have been a problem, as a two channel conditioner was the only one available.

The air temperature rose significantly during the course of a test run which affected the axial reading, although temperature compensation had been designed into each component. With one of the wind tunnel drive fans missing, the turbulence level was higher than desired and this raised the air temperature as much as 10 degrees in a 10 minute run at a Q of 70 psf. This rise was not as significant for the lower Q's, with a rise of 2 or 3 degrees for the same amount of time. Data collection was limited to runs of 10 minutes or less for a Q of 70 psf.

Blockage was not considered a factor requiring correction for two reasons. Initially, the total blocking factor was estimated to be 0.00833, a product of the model frontal area (64 sq. in.) divided by tunnel cross-sectional area (1920 sq. in.) times 1/4 [Ref. 5: p. 9-4]. As each model was similar in cross-section and differed only slightly for the small AOA's considered, it was felt a correction was not necessary. Also an initial test of the change in airspeed due to a change in AOA from 0 to +8 degrees, e.g., was found to be very small, on the order of 3%.

This was measured with a Pitot tube mounted at the cross-sectional location of the model, 6 inches from the tunnel wall.

The output of the balance was considered to be unacceptable in that the drag should have been relatively high for +8 and -10 degrees and low for AOA's near zero. This was not the case, which was attributed to the asymmetrical design of the axial component which produced an unpredictable output. At any AOA other than zero degrees, the balance is influenced by nonlinear strains that produce nonlinear readings. The typical 'bucket', found on graphs of C_d versus AOA was not present (Figure B.1) indicating incorrect results.

B. QUALITATIVE

The flow visualization technique of cotton tufting was adequate to distinguish a difference in flows between various model combinations, but not between different Q's (30 and 70) for a particular model. This can be attributed to the insensitivity of the relatively heavy tufting material and the tape used to secure it. The boundary layer was influenced enough by the material to produce a turbulent boundary layer farther towards the nose than would have otherwise occurred. This influence was strong enough to eliminate the subtle differences that would have been present for the narrow band of Reynolds numbers that were tested. For a given model there was no difference distinguishing the tufted photographs for two different airspeeds, as one would expect. For this reason only one set of photographs, covering both Q's was included (Figures C.1-C.9).

The concept of Mini-tufting was tested to determine whether or not the existing strobe was powerful enough to illuminate the model. Figure A.12 depicts the layout used to photograph a Mini-tufted airfoil, mounted in place of the model and also gives a listing of the filters used [Ref. 6: p. 16]. The strobe, a General Radio electronic stroboscope, type 1540-P3, was only capable of 10 Joule bursts where 500 joules were required. It was felt that the higher flash rates this strobe is capable of would provide enough light over the 1/30th second

exposure needed to 'freeze' the tufts. A roll of Tri-X film was pushed to 1200 ASA and exposed at F3.5 from 1/60th second to 10 seconds. This was also done for F5.6 with the outcome expected to be a bracketing of the correct amount of light. The resulting photographs are not included as none showed anything more than slight shadows of the photographed airfoil.

V. CONCLUSIONS AND RECOMMENDATIONS

A. CONCLUSIONS

The experimental apparatus designed and built to support this thesis was adequate to recommend further research. The pitching moment and normal component of the balance produced reliable output, especially the normal component. The axial component, on the other hand, was not sufficiently accurate and requires redesigning. A possible design to produce linear strain in the axial component is included in Figure 5.1

The tufting used was useful for visualizing the flow for a given model, but must be improved for comparing different models. The 'Mini-tufting' technique would be excellent in that it is non-intrusive and sensitive to small flow differences.

The graphical output was not accurate as a result of the balance data being erroneous. The axial component proved to be consistent but inaccurate and, as lift and drag readings are dependent upon this, the graphs are not helpful.

The flow visualization was adequate for indicating trends between model types, but determining nuances in the flow was found to be very difficult. Analyzing photos of a particular model for a given AOA, at different Q's resulted in no visible differences in the flow.

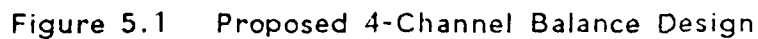
B. RECOMMENDATIONS

The following are given as recommendations to improve the accuracy of data and to decrease the time spent collecting data. Recommendations are listed in order of importance with the most important being first.

1. *Design/construct new balance.* The original design was found to be acceptable with respect to the normal and pitching moment channel but not the axial, due to the asymmetrical

design of that component. This resulted from the diameter of the balance at the axial location being too small. If this portion of the balance was thickened, a symmetric component could be designed. Figure 5.1 contains a possible design for such a balance with the inclusion of a yawing moment channel. This design allows for minimum remachining of the common fuselage. The strain gages applied to the present balance were for aluminum, but this was considered adequate for this application after having consulted with the strain gage manufacturer. The correct gages, for stainless steel, arrived too late for use, but could be used for a new design and would only improve the accuracy.

2. *Vibration damping system.* The movement of the model in the tunnel was sufficient enough to cause a requirement for signal conditioning. This movement was most likely a result of the stiffness of the sting support in the pitching and yawing planes, and possibly a result of the turbulence present in the test section. A system to damp this vibration would perhaps delete the requirement for signal conditioning. Figures 5.2 and 5.3 contain possible designs for such a vibration damping mechanism.
3. *Strobe for Mini-tufting.* An effort was made to use an existing low-powered electronic strobe to illuminate the models for photographing with Mini-tufts. The strobe was inadequate, but one powerful enough is available and would be a great improvement over the technique of flow visualization that was used. Reference 8 tufts describes the correct strobe, use of equipment, and gives ordering information.
4. *Thrust bearings for drive gear.* At times the current required to drive the sting was excessive requiring a change in the testing procedure to prevent the motor from overheating. The fact that thrust washers were used in the drive mechanism, instead of thrust bearings, is a likely cause of the increase in friction that resulted. Remachining the drive gear and



5. *Drive rod replacement.* To ensure that the sting support was available for early use, the drive rod used was a common threaded rod and not one with ACME threads. An ACME thread, where 90 degree thread faces, not angled faces are present, reduces the amount of friction as well as the torque

LEAD SHOT VIBRATION DAMPER

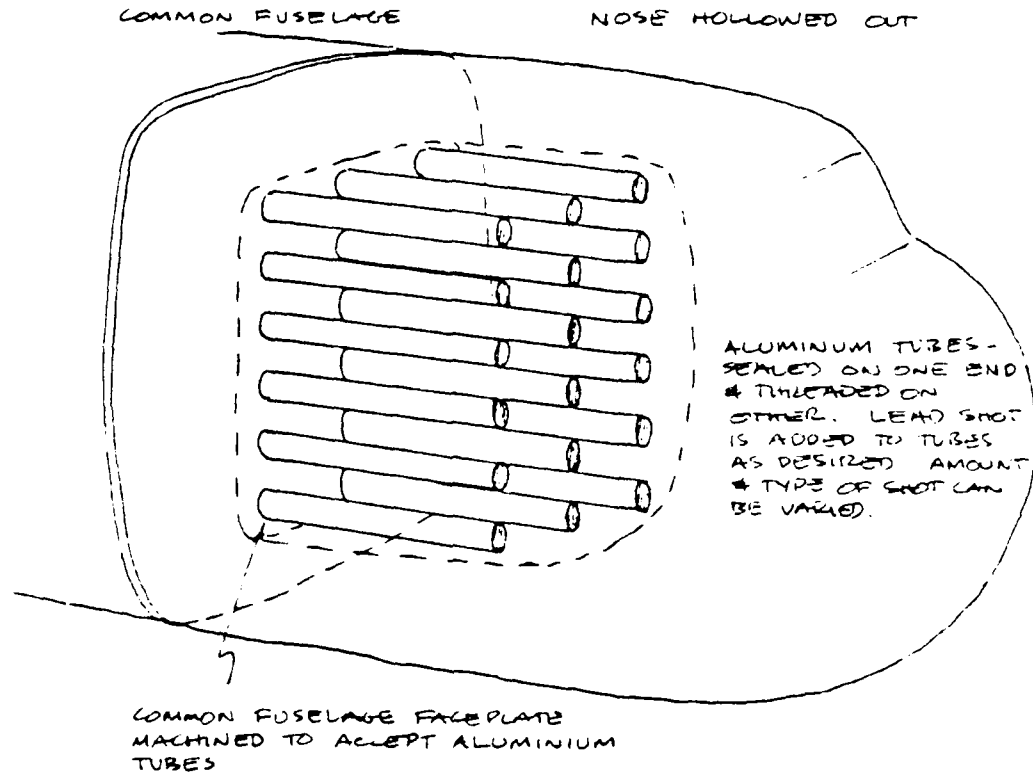


Figure 5.2 Vibration Damping System, 1st Design

required to drive the rod. The drive rod should be replaced to lower friction in the drive train.

6. *Drive motor.* The AOA drive motor was found to be too weak to drive the sting for prolonged periods without overheating. A capacitive start, 1/3 horsepower, reversing motor would increase the rate of AOA change, reducing the amount of time lost between data points and ensuring a longer life for the drive system.
7. *AOA limit switches.* No provisions were made to prevent the drive mechanism from jamming the sting support in the full up or full down position. This in fact did occur, but fortunately

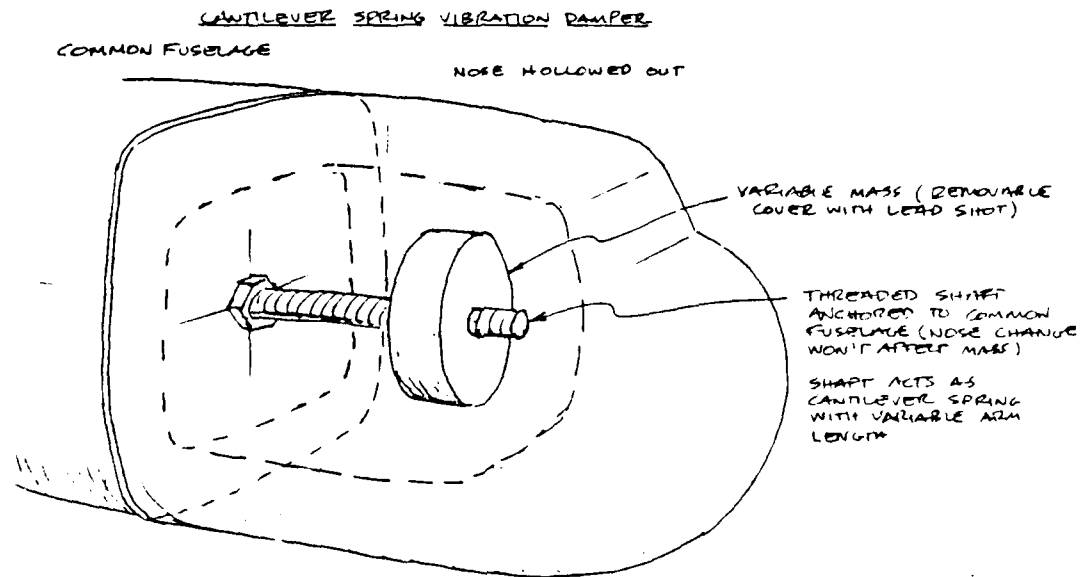


Figure 5.3 Vibration Damping System, 2nd Design

no damage was done. To prevent permanent damage limit switches in the form of DC relays could be installed on the sting support at the limit of travel.

8. *Signal conditioning.* Signal conditioning proved helpful for the axial and normal channels and would most likely help for any additional channels used in the future. The AOA readout was readable without any conditioning, but it would have helped. The fact that only a two channel conditioner was available prevented any other channels from being conditioned.
9. *Pitching moment strain gages.* The strain gages for the pitching moment component were mounted to provide for

temperature compensation, but in an inefficient way. If the two gages perpendicular to the longitudinal axis of the model were reapplied parallel to this axis, the output would double and temperature compensation would still be present.

10. *Axial component strain gages.* The readout of the axial component tended to drift during initial use of the balance. This was diagnosed as a gage that had peeled slightly, causing a change in the balancing of the Wheatstone bridge prior to use. Fortunately this condition was not present during testing, a result of the peeling having stopped. To ensure consistency in the axial component, the axial gages should be replaced.
11. *Computer program.* Many FORTRAN computer programs were written and modified to produce the graphical output used in this thesis. A more efficient approach would consolidate these programs into one that would contain the graphics programs as subroutines, requiring simple prompting prior to each run to produce the desired output.
12. *Wind tunnel survey.* The wind tunnel used is known to have poor test section conditions, mainly a result of the removal of one set of drive props and a shortened diffuser section which causes flow separation. But other problems exist as well and a complete tunnel survey would enable cost effective repair when funds become available. A survey would measure turbulence, velocity, and angularity in the test section at a range of tunnel speeds.
13. Those following this thesis should examine the effects of tunnel wall corrections and incorporate these into the computer program.

APPENDIX A
TABLES, FIGURES, AND PROGRAMS

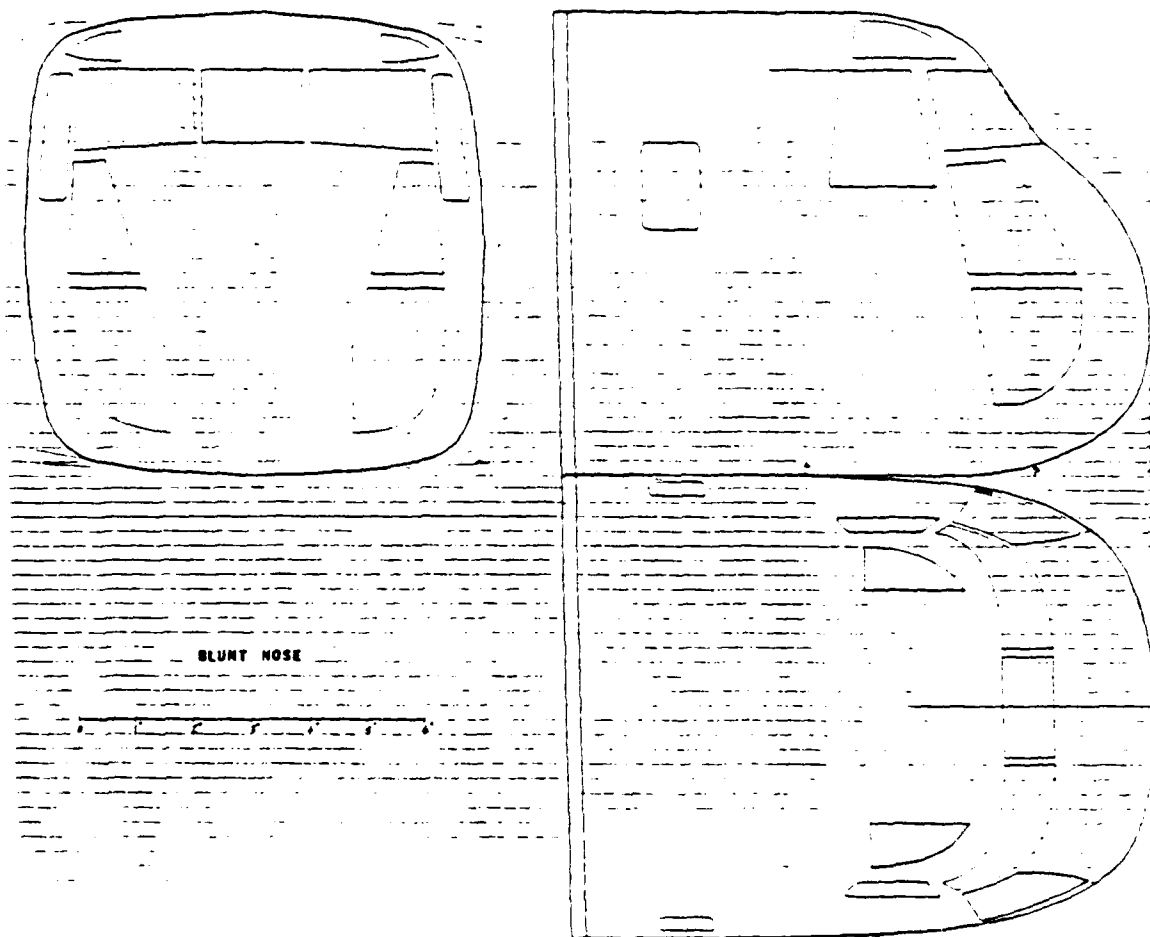


Figure A.1 Planview of Blunt Nose

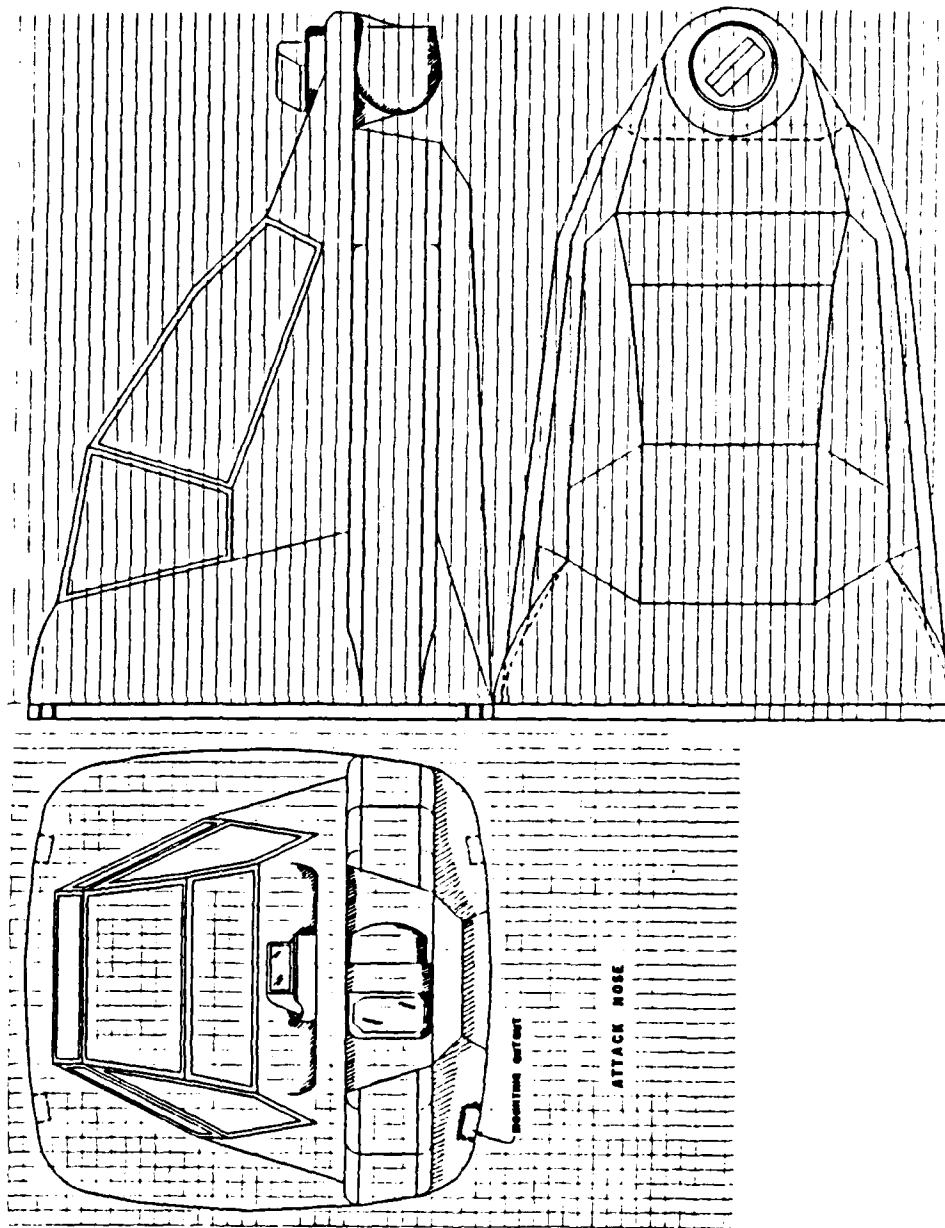


Figure A.2 Planview of Attack Nose

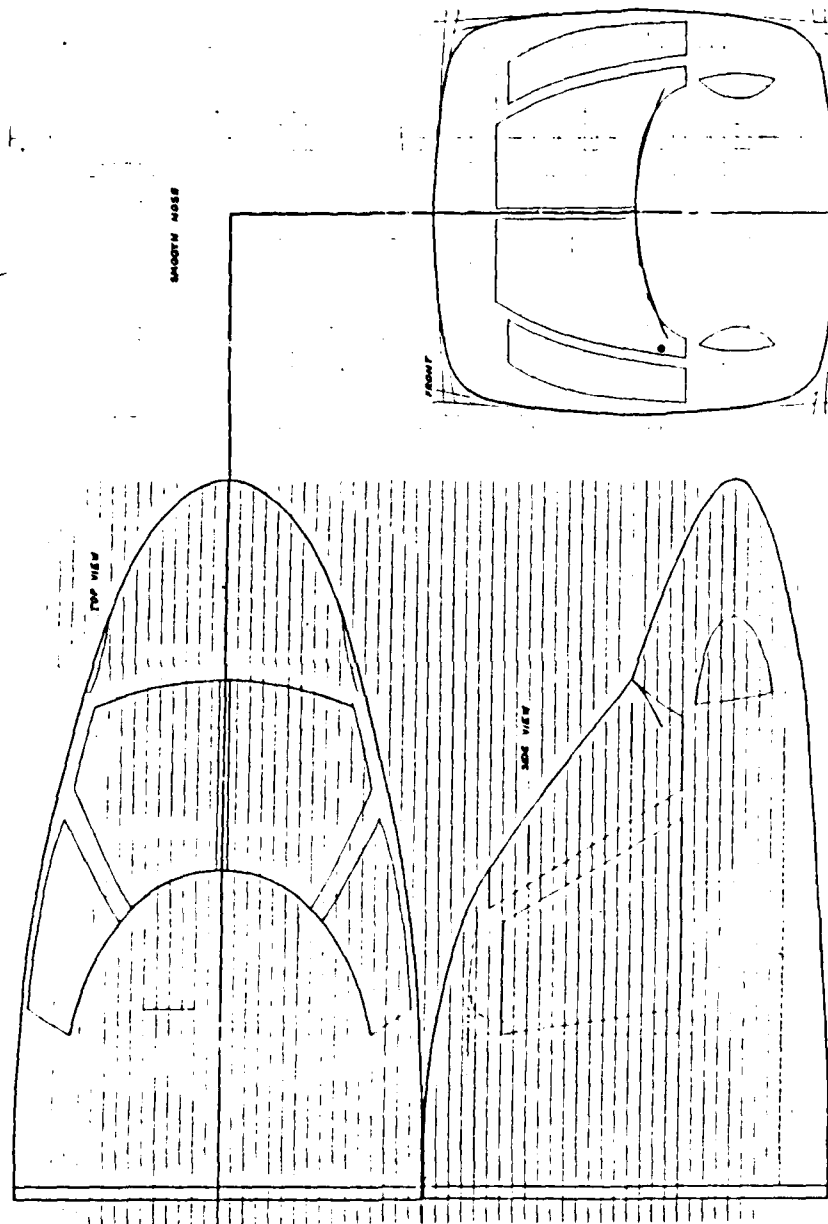


Figure A.3 Planview of Smooth Nose

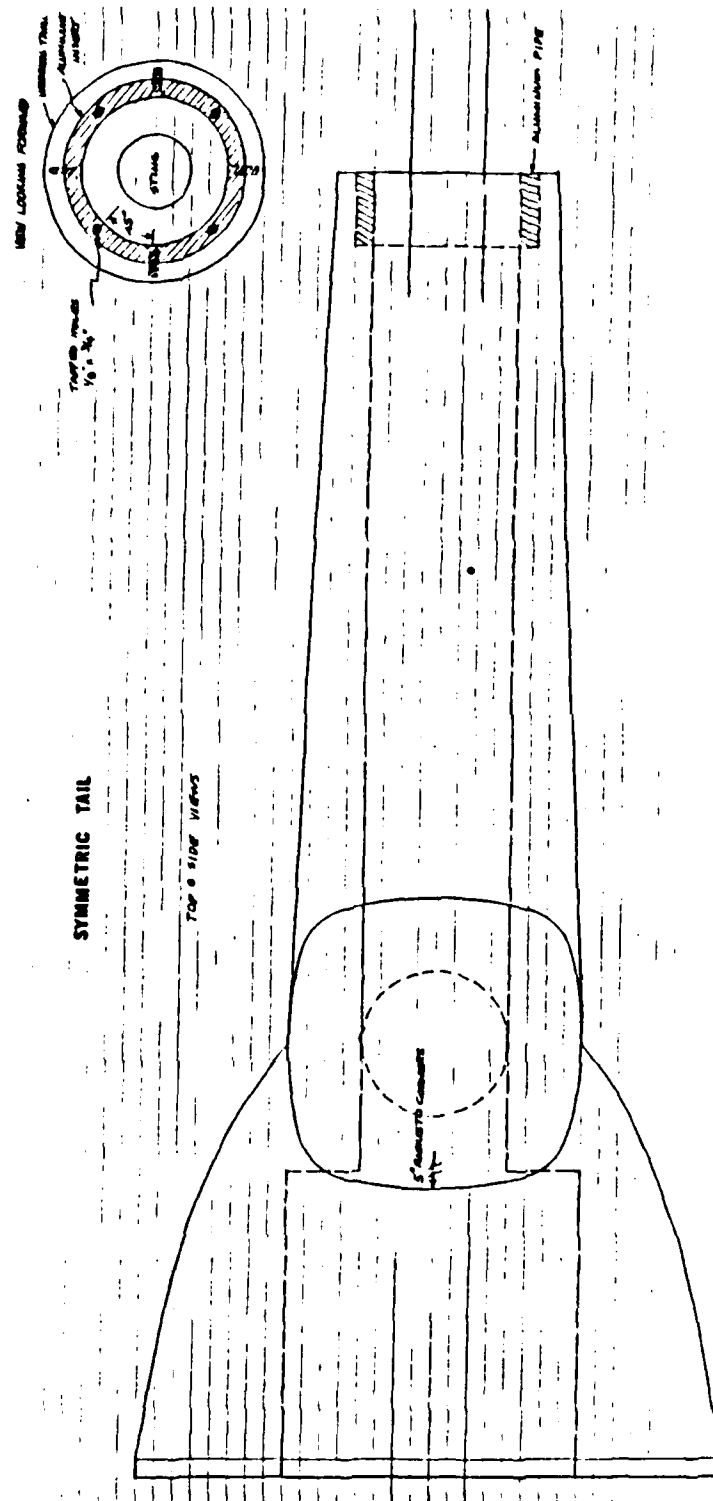


Figure A.4 Planview of Symmetric Tail

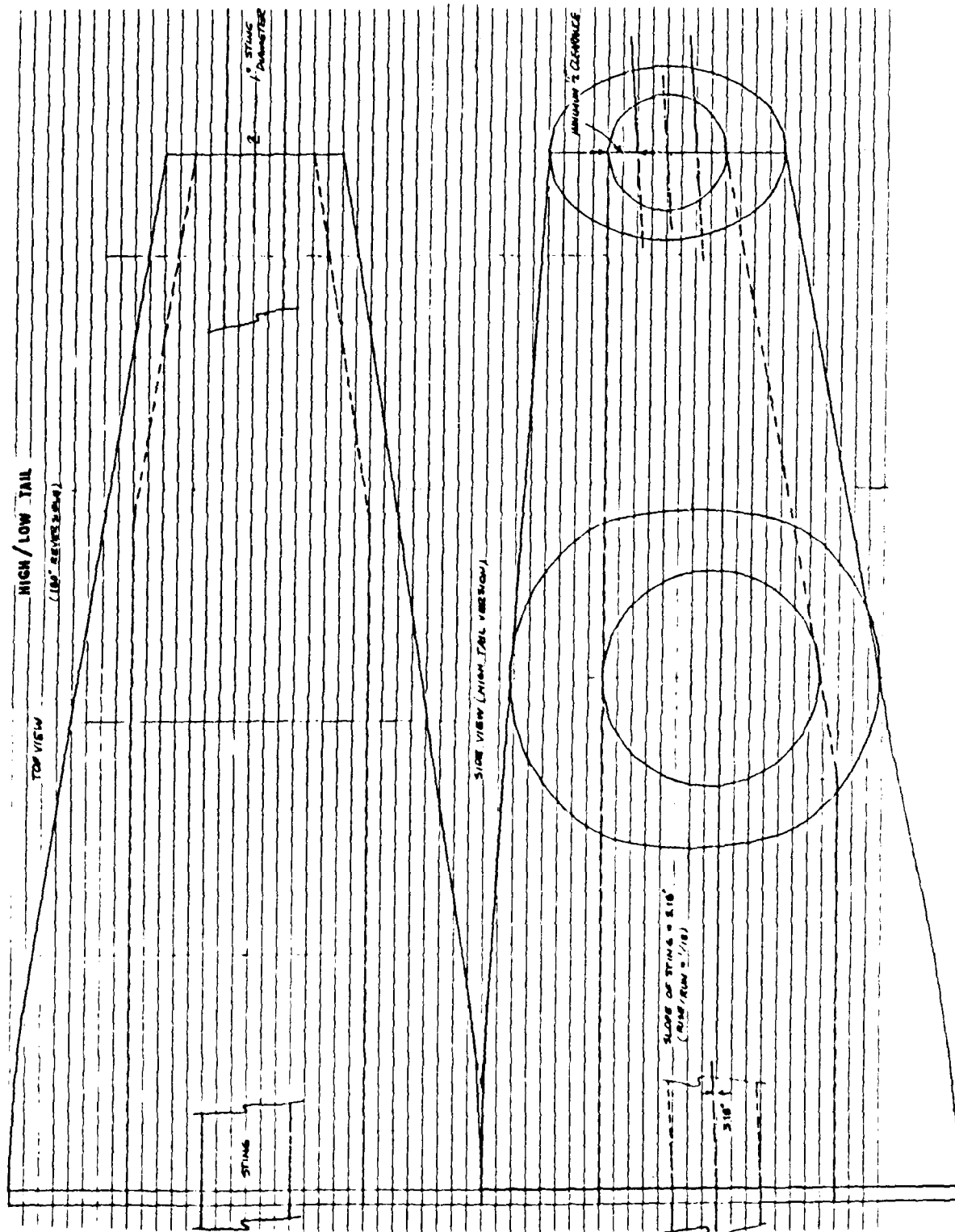


Figure A.5 Planview of High/Low Tail

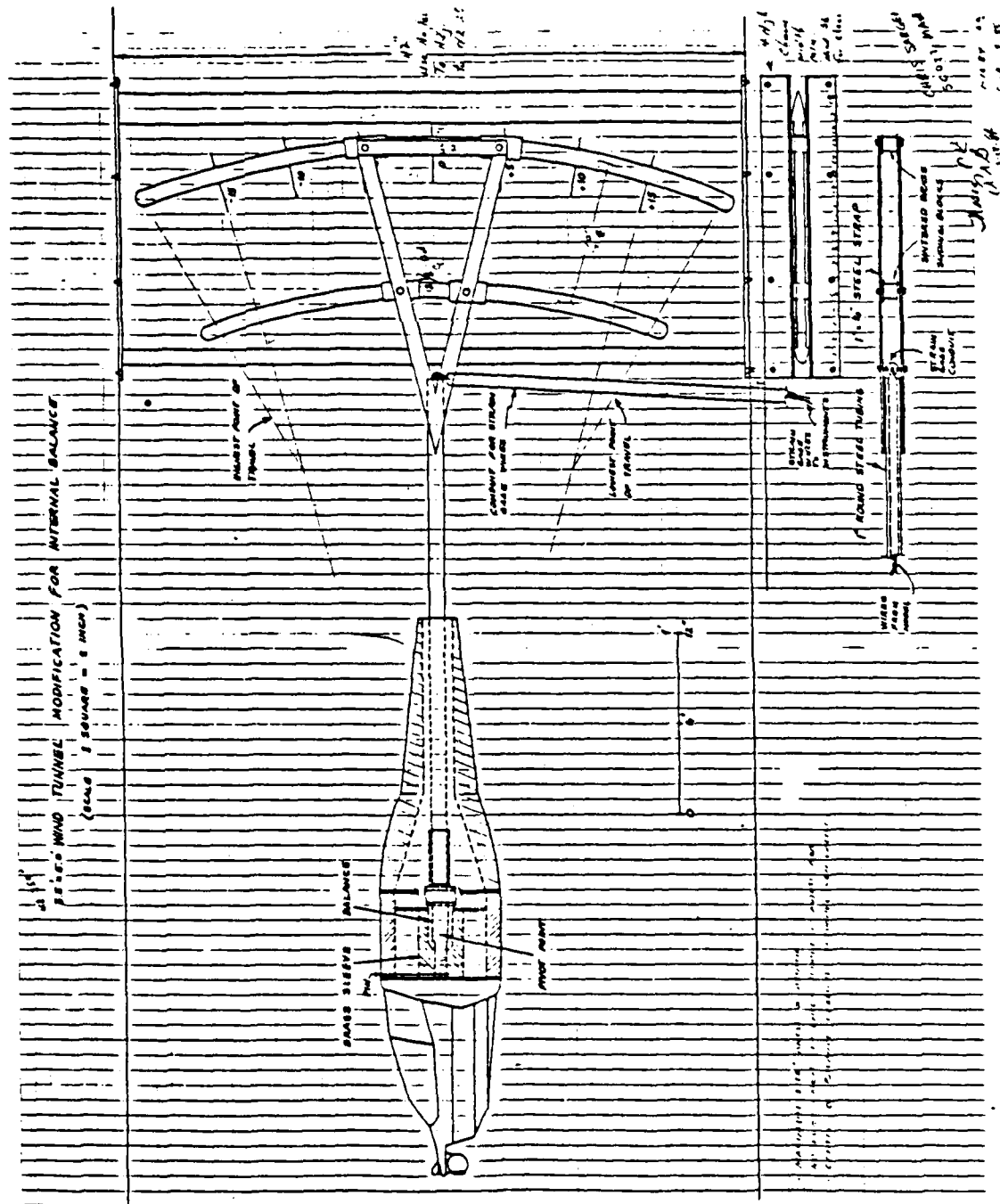


Figure A.7 Planview of Sting Support System

NOSE/TAIL=1/ REMARKS: RUN#1 ATTACK/HIGH
 NORMAL AXIAL
 100/ 100/ (CORRECTION FACTOR)
 0/ 0/ (AFTER-RUN OFF-ZERO READING)

O=10		
NOSE	TAIL	AXIAL
8/	6/	32/
6/	3/	23/
4/	-1/	20/
2/	-2/	8/
0/	-5/	2/
-2/	-8/	-3/
-4/	-9/	-12/
-6/	-10/	-22/
-8/	-12/	-30/
-10/	-14/	-45/
O=30		
NOSE	TAIL	AXIAL
8/	20/	60/
6/	13/	50/
4/	5/	42/
2/	-1/	30/
0/	-10/	20/
-2/	-18/	10/
-4/	-25/	0/
-6/	-30/	-10/
-8/	-41/	-21/
-10/	-50/	-35/
O=50		
NOSE	TAIL	AXIAL
8/	34/	30/
6/	17/	80/
4/	5/	74/
2/	-5/	62/
0/	-10/	53/
-2/	-30/	45/
-4/	-42/	35/
-6/	-57/	23/
-8/	-70/	10/
-10/	-80/	-3/
O=70		
NOSE	TAIL	AXIAL
8/	50/	92/
6/	31/	90/
4/	11/	71/
2/	-7/	56/
0/	-24/	40/
-2/	-42/	25/
-4/	-60/	18/
-6/	-80/	-4/
-8/	-104/	-38/
-10/	-127/	-45/

Figure A.8 Raw Data Files

NOSE/TALE=2/			REMARKS: RUN#1_ATTACK/MIDDLE		
NORMAL			AXIAL		
100/			100/		
0/			(CORRECTION FACTOR)		
			(AFTER-RUN OFF-ZERO READING)		
-----O=10-----					
AOA	NORMAL	AXIAL			
8/	0/	41/			
6/	6/	29/			
4/	0/	23/			
2/	-1/	14/			
0/	-3/	6/			
-2/	-4/	0/			
-4/	-5/	-7/			
-6/	-8/	-19/			
-8/	-9/	-26/			
-10/	-12/	-34/			
-----O=30-----					
AOA	NORMAL	AXIAL			
8/	21/	55/			
6/	11/	43/			
4/	6/	40/			
2/	0/	30/			
0/	-8/	20/			
-2/	-14/	13/			
-4/	-20/	6/			
-6/	-26/	-5/			
-8/	-35/	-12/			
-10/	-48/	-29/			
-----O=50-----					
AOA	NORMAL	AXIAL			
8/	34/	78/			
6/	21/	73/			
4/	8/	63/			
2/	0/	55/			
0/	-12/	43/			
-2/	-21/	43/			
-4/	-33/	35/			
-6/	-46/	29/			
-8/	-60/	12/			
-10/	-77/	0/			
-----O=70-----					
AOA	NORMAL	AXIAL			
8/	50/	99/			
6/	30/	80/			
4/	15/	70/			
2/	1/	54/			
0/	-15/	45/			
-2/	-31/	25/			
-4/	-46/	15/			
-6/	-65/	6/			
-8/	-92/	-15/			
-10/	-115/	-37/			

Figure A.8 Raw Data Files(cont'd)

NOSE/TALE=3/		REMARKS: RUN#1 <u>ATTACK / LOW</u>	
NORMAL	AXIAL	(CORRECTION FACTOR)	
98/	98/	(AFTER-PIN OFF-2520 READING)	
0/	0/	Q=10	
AOA	NORMAL	AXIAL	
8/	11/	42/	
6/	7/	30/	
4/	4/	22/	
2/	0/	8/	
0/	-2/	-3/	
-2/	-4/	-7/	
-4/	-6/	-15/	
-6/	-7/	-27/	
-8/	-9/	-38/	
-10/	-11/	-48/	
Q=30			
AOA	NORMAL	AXIAL	
8/	30/	55/	
6/	22/	48/	
4/	13/	33/	
2/	5/	27/	
0/	-1/	14/	
-2/	-6/	6/	
-4/	-15/	2/	
-6/	-21/	-13/	
-8/	-32/	-28/	
-10/	-39/	-40/	
Q=50			
AOA	NORMAL	AXIAL	
8/	50/	82/	
6/	36/	73/	
4/	20/	62/	
2/	8/	46/	
0/	-2/	36/	
-2/	-14/	20/	
-4/	-27/	13/	
-6/	-37/	-3/	
-8/	-54/	-15/	
-10/	-68/		
Q=70			
AOA	NORMAL	AXIAL	
8/	71/	90/	
6/	51/	80/	
4/	29/	75/	
2/	10/	60/	
0/	-8/	40/	
-2/	-23/	27/	
-4/	-45/	10/	
-6/	-60/	-3/	
-8/	-82/	-10/	
-10/	-104/	-50/	

Figure A.8 Raw Data Files(cont'd)

NOSE/TAIL=4/			REMARKS: RUN#1 BLUNT/HIGH		
NORMAL AXIAL			(CORRECTION FACTOR)		
100/ 99/			(AFTER-PIN OFF-ZERO READING)		
0/ 0/			-----		
Q=10			-----		
AOA	NORMAL	AXIAL			
8/	9/	40/			
6/	3/	20/			
4/	0/	23/			
2/	-2/	10/			
0/	-4/	7/			
-2/	-8/	-4/			
-4/	-10/	-10/			
-6/	-12/	-18/			
-8/	-15/	-22/			
-10/	-17/	-35/			
Q=20			-----		
AOA	NORMAL	AXIAL			
8/	30/	55/			
6/	20/	50/			
4/	12/	40/			
2/	4/	32/			
0/	-4/	22/			
-2/	-12/	14/			
-4/	-10/	4/			
-6/	-20/	-5/			
-8/	-34/	-15/			
-10/	-47/	-25/			
Q=50			-----		
AOA	NORMAL	AXIAL			
8/	43/	80/			
6/	32/	79/			
4/	19/	70/			
2/	6/	65/			
0/	-5/	57/			
-2/	-20/	41/			
-4/	-32/	30/			
-6/	-45/	22/			
-8/	-59/	13/			
-10/	-73/	0/			
Q=70			-----		
AOA	NORMAL	AXIAL			
8/	65/	110/			
6/	43/	100/			
4/	22/	94/			
2/	6/	73/			
0/	-8/	62/			
-2/	-30/	40/			
-4/	-40/	23/			
-6/	-68/	10/			
-8/	-89/	0/			
-10/	-108/	-15/			

Figure A.8 Raw Data Files(cont'd)

REMARKS: DUN41 BLUNT/41001P		
(CORRECTION FACTOR)		
(AFTER-RUN OFF-ZERO READING)		
Q=10		
AOA	NORMAL	AXIAL
8/	8/	33/
6/	8/	28/
4/	1/	22/
2/	-1/	13/
0/	-2/	5/
-2/	-4/	-3/
-4/	-7/	-9/
-6/	-8/	-22/
-8/	-10/	-30/
-10/	-11/	-37/
Q=30		
AOA	NORMAL	AXIAL
8/	24/	50/
6/	16/	42/
4/	8/	40/
2/	3/	30/
0/	-3/	21/
-2/	-10/	13/
-4/	-17/	0/
-6/	-25/	-10/
-8/	-32/	-24/
-10/	-40/	-34/
Q=50		
AOA	NORMAL	AXIAL
8/	47/	83/
6/	30/	79/
4/	18/	67/
2/	6/	58/
0/	-2/	45/
-2/	-15/	36/
-4/	-23/	13/
-6/	-40/	2/
-8/	-53/	-5/
-10/	-68/	-22/
Q=70		
AOA	NORMAL	AXIAL
8/	53/	126/
6/	44/	108/
4/	27/	96/
2/	10/	75/
0/	-3/	62/
-2/	-21/	40/
-4/	-42/	20/
-6/	-61/	0/
-8/	-78/	-4/
-10/	-101/	-20/

Figure A.8 Raw Data Files(cont'd)

NOSE/TAIL=6/		REMARKS: RUN#1 BLUNT/LOW	
NORMAL	AXIAL	(CORRECTION FACTOR)	
100/	100/	(AFTER-FCIN OFF-ZERO READING)	
0/	0/	Q=10	
AOA	NORMAL	AXIAL	
8/	11/	47/	
6/	7/	40/	
4/	4/	30/	
2/	1/	22/	
0/	-1/	15/	
-2/	-3/	5/	
-4/	-5/	0/	
-6/	-7/	-5/	
-8/	-8/	-13/	
-10/	-9/	-25/	
		Q=30	
AOA	NORMAL	AXIAL	
8/	36/	56/	
6/	24/	48/	
4/	17/	40/	
2/	10/	30/	
0/	2/	21/	
-2/	-6/	12/	
-4/	-13/	3/	
-6/	-20/	-3/	
-8/	-30/	-17/	
-10/	-37/	-25/	
		Q=50	
AOA	NORMAL	AXIAL	
8/	50/	85/	
6/	43/	75/	
4/	35/	65/	
2/	20/	56/	
0/	6/	47/	
-2/	-3/	38/	
-4/	-17/	30/	
-6/	-30/	20/	
-8/	-45/	3/	
-10/	-53/	0/	
		Q=70	
AOA	NORMAL	AXIAL	
8/	87/	94/	
6/	63/	84/	
4/	40/	70/	
2/	28/	59/	
0/	5/	40/	
-2/	-12/	20/	
-4/	-30/	3/	
-6/	-50/	-10/	
-8/	-60/	-23/	
-10/	-92/	-45/	

Figure A.8 Raw Data Files(cont'd)

NOSE/TAIL=7/		REMARKS: RUN#1_SMOOTH/HIGH	
NORMAL		AXIAL	
100/		100/	
0/		0/	
		(CORRECTION FACTOR)	
		(AFTER-PTN OFF-ZERO READING)	

C=10			
AOA	NORMAL	AXIAL	
8/	8/	40/	
6/	4/	34/	
4/	1/	26/	
2/	-2/	20/	
0/	-6/	7/	
-2/	-9/	2/	
-4/	-10/	-4/	
-6/	-13/	-13/	
-8/	-16/	-23/	
-10/	-18/	-32/	

C=30			
AOA	NORMAL	AXIAL	
8/	15/	44/	
6/	3/	33/	
4/	1/	22/	
2/	-2/	19/	
0/	-8/	7/	
-2/	-15/	-3/	
-4/	-10/	-13/	
-6/	-25/	-22/	
-8/	-30/	-33/	
-10/	-37/	-43/	

C=50			
AOA	NORMAL	AXIAL	
8/	42/	92/	
6/	27/	78/	
4/	13/	70/	
2/	1/	63/	
0/	-13/	45/	
-2/	-26/	35/	
-4/	-41/	17/	
-6/	-56/	3/	
-8/	-70/	-8/	
-10/	-82/	-20/	

C=70			
AOA	NORMAL	AXIAL	
8/	65/	114/	
6/	39/	90/	
4/	20/	80/	
2/	0/	58/	
0/	-20/	45/	
-2/	-40/	25/	
-4/	-63/	5/	
-6/	-84/	-12/	
-8/	-105/	-23/	
-10/	-123/	-37/	

Figure A.8 Raw Data Files(cont'd)

NOISE/TALE=2/			REMARKS: RUN#1_SMOOTH/MIDDLE		
NORMAL AXIAL			(CORRECTION FACTOR)		
100/ 100/			(AFTER-RUN OFF-ZERO READING)		
0/ 0/			-----		
Q=11			-----		
AOA	NORMAL	AXIAL			
8/	6/	38/			
6/	4/	32/			
4/	0/	20/			
2/	-1/	12/			
0/	-5/	4/			
-2/	-6/	-2/			
-4/	-10/	-13/			
-6/	-10/	-20/			
-8/	-12/	-30/			
-10/	-13/	-40/			
Q=30			-----		
AOA	NORMAL	AXIAL			
8/	27/	65/			
6/	19/	50/			
4/	9/	48/			
2/	3/	38/			
0/	-3/	24/			
-2/	-11/	15/			
-4/	-21/	2/			
-6/	-32/	-3/			
-8/	-30/	-18/			
-10/	-49/	-39/			
Q=50			-----		
AOA	NORMAL	AXIAL			
8/	36/	87/			
6/	23/	78/			
4/	10/	67/			
2/	-2/	58/			
0/	-13/	42/			
-2/	-27/	33/			
-4/	-40/	17/			
-6/	-53/	3/			
-8/	-67/	-5/			
-10/	-83/	-22/			
Q=70			-----		
AOA	NORMAL	AXIAL			
8/	55/	111/			
6/	39/	99/			
4/	16/	70/			
2/	1/	61/			
0/	-15/	42/			
-2/	-35/	25/			
-4/	-56/	3/			
-6/	-80/	-13/			
-8/	-102/	-28/			
-10/	-121/	-55/			

Figure A.8 Raw Data Files(cont'd)

NOSE/TALE=2/		REMARKS: RUN#1_SMOOTH/104	
NORMAL	AXIAL	(CORRECTION FACTOR)	
98/	100/	(AFTER-RUN OFF-ZERO READING)	
0/	0/		
-----Q=10-----			
AOA	NORMAL	AXIAL	
8/	12/	42/	
6/	9/	29/	
4/	5/	20/	
2/	2/	7/	
0/	0/	2/	
-2/	-2/	-7/	
-4/	-4/	-10/	
-6/	-6/	-24/	
-8/	-7/	-38/	
-10/	-9/	-45/	
-----Q=30-----			
AOA	NORMAL	AXIAL	
8/	38/	60/	
6/	29/	52/	
4/	20/	40/	
2/	10/	29/	
0/	4/	18/	
-2/	-2/	2/	
-4/	-12/	-12/	
-6/	-21/	-22/	
-8/	-30/	-33/	
-10/	-36/	-47/	
-----Q=50-----			
AOA	NORMAL	AXIAL	
8/	53/	83/	
6/	44/	77/	
4/	27/	63/	
2/	14/	54/	
0/	1/	39/	
-2/	-13/	26/	
-4/	-29/	18/	
-6/	-43/	3/	
-8/	-57/	-12/	
-10/	-72/	-29/	
-----Q=70-----			
AOA	NORMAL	AXIAL	
8/	83/	100/	
6/	67/	90/	
4/	40/	80/	
2/	19/	54/	
0/	0/	35/	
-2/	-21/	20/	
-4/	-42/	0/	
-6/	-64/	-21/	
-8/	-84/	-42/	
-10/	-105/	-65/	

Figure A.8 Raw Data Files(cont'd)

TABLE 1
Balance Calibration Data, Normal Component

																				POUNDS OF NORMAL FORCE
0	1	2	3	4	5	6	7	8	9	10	11	12	13	14	15	16	17	18	19	
200	191	181	171	161	151	141	131	121	111	101	91	81	71	61	51	41	31	21	11	0
190	180	170	160	150	140	130	120	110	100	90	80	70	60	50	40	30	20	10	0	-10
180	170	160	150	140	130	120	110	100	90	80	70	60	50	40	30	20	10	0	-10	-20
170	160	150	140	130	120	110	100	90	80	70	60	50	40	30	20	10	0	-10	-20	-30
160	150	140	130	120	110	100	90	80	70	60	50	40	30	20	10	0	-10	-20	-30	-40
150	140	130	120	110	100	90	80	70	60	50	40	30	20	10	0	-10	-20	-30	-40	-50
140	130	120	110	100	90	80	70	60	50	40	30	20	10	0	-10	-20	-30	-40	-50	-60
130	120	110	100	90	80	70	60	50	40	30	20	10	0	-10	-20	-30	-40	-50	-60	-70
120	110	100	90	80	70	60	50	40	30	20	10	0	-10	-20	-30	-40	-50	-60	-70	-80
110	100	90	80	70	60	50	40	30	20	10	0	-10	-20	-30	-40	-50	-60	-70	-80	-90
100	90	80	70	60	50	40	30	20	10	0	-10	-20	-30	-40	-50	-60	-70	-80	-90	-100
90	80	70	60	50	40	30	20	10	0	-10	-20	-30	-40	-50	-60	-70	-80	-90	-100	-110
80	70	60	50	40	30	20	10	0	-10	-20	-30	-40	-50	-60	-70	-80	-90	-100	-110	-120
70	60	50	40	30	20	10	0	-10	-20	-30	-40	-50	-60	-70	-80	-90	-100	-110	-120	-130
60	50	40	30	20	10	0	-10	-20	-30	-40	-50	-60	-70	-80	-90	-100	-110	-120	-130	-140
50	40	30	20	10	0	-10	-20	-30	-40	-50	-60	-70	-80	-90	-100	-110	-120	-130	-140	-150
40	30	20	10	0	-10	-20	-30	-40	-50	-60	-70	-80	-90	-100	-110	-120	-130	-140	-150	-160
30	20	10	0	-10	-20	-30	-40	-50	-60	-70	-80	-90	-100	-110	-120	-130	-140	-150	-160	-170
20	10	0	-10	-20	-30	-40	-50	-60	-70	-80	-90	-100	-110	-120	-130	-140	-150	-160	-170	-180
10	0	-10	-20	-30	-40	-50	-60	-70	-80	-90	-100	-110	-120	-130	-140	-150	-160	-170	-180	-190
0	-10	-20	-30	-40	-50	-60	-70	-80	-90	-100	-110	-120	-130	-140	-150	-160	-170	-180	-190	-200
-10	-20	-30	-40	-50	-60	-70	-80	-90	-100	-110	-120	-130	-140	-150	-160	-170	-180	-190	-200	-210
-20	-30	-40	-50	-60	-70	-80	-90	-100	-110	-120	-130	-140	-150	-160	-170	-180	-190	-200	-210	-220
-30	-40	-50	-60	-70	-80	-90	-100	-110	-120	-130	-140	-150	-160	-170	-180	-190	-200	-210	-220	-230
-40	-50	-60	-70	-80	-90	-100	-110	-120	-130	-140	-150	-160	-170	-180	-190	-200	-210	-220	-230	-240
-50	-60	-70	-80	-90	-100	-110	-120	-130	-140	-150	-160	-170	-180	-190	-200	-210	-220	-230	-240	-250
-60	-70	-80	-90	-100	-110	-120	-130	-140	-150	-160	-170	-180	-190	-200	-210	-220	-230	-240	-250	-260
-70	-80	-90	-100	-110	-120	-130	-140	-150	-160	-170	-180	-190	-200	-210	-220	-230	-240	-250	-260	-270
-80	-90	-100	-110	-120	-130	-140	-150	-160	-170	-180	-190	-200	-210	-220	-230	-240	-250	-260	-270	-280
-90	-100	-110	-120	-130	-140	-150	-160	-170	-180	-190	-200	-210	-220	-230	-240	-250	-260	-270	-280	-290
-100	-110	-120	-130	-140	-150	-160	-170	-180	-190	-200	-210	-220	-230	-240	-250	-260	-270	-280	-290	-300
-110	-120	-130	-140	-150	-160	-170	-180	-190	-200	-210	-220	-230	-240	-250	-260	-270	-280	-290	-300	-310
-120	-130	-140	-150	-160	-170	-180	-190	-200	-210	-220	-230	-240	-250	-260	-270	-280	-290	-300	-310	-320
-130	-140	-150	-160	-170	-180	-190	-200	-210	-220	-230	-240	-250	-260	-270	-280	-290	-300	-310	-320	-330
-140	-150	-160	-170	-180	-190	-200	-210	-220	-230	-240	-250	-260	-270	-280	-290	-300	-310	-320	-330	-340
-150	-160	-170	-180	-190	-200	-210	-220	-230	-240	-250	-260	-270	-280	-290	-300	-310	-320	-330	-340	-350
-160	-170	-180	-190	-200	-210	-220	-230	-240	-250	-260	-270	-280	-290	-300	-310	-320	-330	-340	-350	-360
-170	-180	-190	-200	-210	-220	-230	-240	-250	-260	-270	-280	-290	-300	-310	-320	-330	-340	-350	-360	-370
-180	-190	-200	-210	-220	-230	-240	-250	-260	-270	-280	-290	-300	-310	-320	-330	-340	-350	-360	-370	-380
-190	-200	-210	-220	-230	-240	-250	-260	-270	-280	-290	-300	-310	-320	-330	-340	-350	-360	-370	-380	-390
-200	-210	-220	-230	-240	-250	-260	-270	-280	-290	-300	-310	-320	-330	-340	-350	-360	-370	-380	-390	-400

THIS TABLE INDICATES THE 'NORMAL' READOUT, IN COUNTS, WHEN THE BALANCE WAS LOADED UNDER THE ABOVE CONDITIONS. THE NEGATIVE OUTPUT WAS HIPORED TO PRODUCE A POSITIVE QUADRANT. THE HAPPING THAT RESULTED WAS USED TO CORRECT THE AXIAL DATA COLLECTED DURING TPST RUNS.

TABLE 2
Balance Calibration Data, Axial Component

[illegible]

THIS TABLE INDICATES THE 'AXIAL' READOUT IN COUNTS. WHEN THE BALANCE WAS LOADED UNDER THE ABOVE CONDITIONS, THE NEGATIVE OUTPUT WAS IMPROVED TO PRODUCE A NEGATIVE QUADRANT. THE MAPPING THAT RESULTED WAS USED TO CORRECT THE NORMAL DATA COLLECTED DURING TEST RUNS.

Figure A.9 FORTRAN Program for Data Conversion(cont'd)

```

CALL XNAME('
CALL YNAME('
CALL XINTAX
CALL YINTAX
CALL GRAF(-12.,2.,12.,-.05,.1,.4)
CALL GRID(1,1)
CALL THKCRV(.02)
DO 101 L = 21,25
IF(L.EQ.22) CALL DASH
IF(L.EQ.23) CALL ECT
CALL CURVES(X,Y,AA,COEFFD,L)
CALL COMCH(5000)
CALL SMCTH
CALL CURVE(X,Y,10,1)
101 CONTINUE
CALL RESET('DCT')
CALL ENDOF(0)
CCCCCCCCCCCCCCCCCCCCCCCCCCCCCCCCCCCCCCCCCCCCCCCCCCCCCCCCCCCC
CALL PHYSCL(2.C,4.7)
CALL AREA2D(5.C,2.5)
CALL MESSAGE('PLUNT DIST S',10,.5,2.0)
CALL XNAME('
CALL YNAME('COEFFICIENT OF DRAGS',100)
CALL XINTAX
CALL YINTAX
CALL RESET('THKCRV')
CALL GRAF(-12.,2.,12.,-.05,.1,.4)
CALL GRID(1,1)
CALL THKCRV(.02)
DO 102 L = 24,26
IF(L.EQ.25) CALL DASH
IF(L.EQ.26) CALL ECT
CALL CURVES(X,Y,AA,COEFFD,L)
CALL CURVE(X,Y,10,1)
102 CONTINUE
CALL RESET('DCT')
CALL ENDOF(0)
CCCCCCCCCCCCCCCCCCCCCCCCCCCCCCCCCCCCCCCCCCCCCCCCCCCCCCCCCCCC
CALL PHYSCL(2.C,1.0)
CALL AREA2D(5.C,2.5)
CALL MESSAGE('SMUTH DIST S',11,.5,2.0)
CALL XNAME('
CALL YNAME('
CALL MESSAGE('ANGLE OF ATTACK(DEGS) S',21,1.0,-0.5)
CALL XINTAX
CALL YINTAX
CALL RESET('THKCRV')
CALL GRAF(-12.,2.,12.,-.05,.1,.4)
CALL GRID(1,1)
CALL THKCRV(.02)
DO 103 L = 27,29
IF(L.EQ.28) CALL DASH
IF(L.EQ.29) CALL ECT
CALL CURVES(X,Y,AA,COEFFD,L)
CALL CURVE(X,Y,10,1)
103 CONTINUE
CALL ENDOF(0)
CALL DASH(8.5,11.0)
CALL SAUSS
CALL SHOCK(90.,1,0.002,1)
CALL PHYSCL(2.C,7.2)
CALL AREA2D(5.C,2.5)
CALL ENDOF(0)
CALL DCEFL
STOP
END

```

Figure A.9 FORTRAN Program for Data Conversion(cont'd)

INTERMEDIATE CALIBRATION AND EQUIPMENT SETUP STEPS

Step No.

1. Turn on all electrical equipment for approximately 10 min.
2. Zero angle of attack reading (AOA).
3. Record model configuration.
4. Install calibration rigging.
5. Zero normal axial component reading on channel #2 amplifier.
6. Zero raw axial component reading on channel #3 amplifier.
7. Zero normal & axial signal conditioner LP adjustment.
8. Place 10 lbs. weight under model on rigging to set Raw normal channel to span of -.0100 counts on voltmeter #1.
RN: -10# = -.0100
9. Check & record conditioned normal signal.
CN: .0100 approximately.
10. Place 10 lbs. weight on axial rigging to set raw axial channel to span of +.0100 on voltmeter #2.
RN: +10# = +.0100
11. Record as counts: conditioned normal (CN).
example: -.0100 is -100 counts.
 conditioned axial (CA).
example: +.0100 is 100 counts.
12. Remove calibration rigging from model.
13. Re-zero angle of attack (AOA).
14. Re-zero raw normal & raw axial channels (should check conditioned normal & conditioned axial to ensure close to raw readings).

Figure A.10 Data Collection Checklist

15. Use DATA RECORD provided and note nose/tail combination number in the first line.
16. Set junction box switches to conditioned normal (CN) and conditioned axial (CA). Both should read ".0000".
17. Ensure all tools and loose equipment is removed from the tunnel and doors are secure.
18. Start tunnel with model at eight degrees AOA.
19. Set Q (speed) of the tunnel. (10,30,50,70)
20. Vary AOA and record counts axial & normal (conditioned).
21. Return model to zero AOA and turn off tunnel motors.
22. Re-zero normal & raw axial channels if necessary.
23. Check and record temperature of the tunnel. Allow tunnel to cool to approximately the same temperature as the start up temperature of the tunnel.
*note: axial channel is very susceptible to large temperature variations.
24. When temperature stabilizes, prepare to continue to next higher Q (speed).
25. Go to step #16 and continue.

Figure A.10 Data Collection Checklist(cont'd)

NOSE/TAIL COMBINATION 1 (ATTACK/HIGH)										
WEIGHT = 24.7 LBS										
Q=10 RE=.175E+07										
AOA	CN	CA	CCN	CCA	IL	LD	CL	CD	REDA	
8	5	33	5	37	3	3	0.020	0.075	0.031	
6	3	33	3	33	1	3	0.013	0.056	0.023	
4	-1	20	0	20	-1	3	-0.007	0.065	0.027	
2	-2	8	-1	8	-1	-1	-0.010	0.016	0.027	
0	-5	-2	-4	3	-4	3	-0.036	0.048	0.020	
-2	-8	-3	-7	-5	-7	5	-0.062	0.165	0.069	
-4	-9	-12	-8	-11	-8	7	-0.073	0.163	0.063	
-6	-10	-23	-3	-21	-10	6	-0.088	0.141	0.059	
-8	-12	-33	-11	-20	-13	7	-0.113	0.172	0.072	
-10	-14	-45	-13	-44	-17	2	-0.150	0.043	0.018	

Q=30 RE=.303E+07										
AOA	CN	CA	CCN	CCA	IL	LD	CL	CD	REDA	
8	20	60	21	61	15	29	0.044	0.232	0.027	
6	13	52	13	53	9	29	0.026	0.226	0.024	
4	6	42	6	41	4	24	0.011	0.193	0.023	
2	-1	30	0	32	-1	23	-0.003	0.187	0.028	
0	-10	20	-9	20	-3	20	-0.027	0.160	0.067	
-2	-18	10	-16	10	-15	19	-0.046	0.153	0.064	
-4	-25	3	-23	2	-22	21	-0.067	0.167	0.069	
-6	-33	-1	-31	-3	-32	20	-0.091	0.161	0.067	
-8	-41	-11	-39	-22	-43	20	-0.117	0.151	0.067	
-10	-50	-35	-49	-36	-51	16	-0.152	0.127	0.053	

Q=50 RE=.501E+07										
AOA	CN	CA	CCN	CCA	IL	LD	CL	CD	REDA	
8	34	80	34	80	24	53	0.042	0.225	0.110	
6	17	80	19	81	12	57	0.021	0.272	0.113	
4	5	74	6	74	1	57	0.003	0.274	0.114	
2	-5	63	-4	62	-6	53	-0.011	0.255	0.126	
0	-10	53	-10	53	-10	52	-0.034	0.239	0.116	
-2	-30	45	-30	46	-27	56	-0.049	0.267	0.111	
-4	-43	35	-43	36	-39	56	-0.070	0.259	0.112	
-6	-57	23	-56	25	-52	57	-0.093	0.271	0.113	
-8	-72	10	-72	14	-67	58	-0.121	0.280	0.117	
-10	-88	-3	-86	-9	-83	49	-0.149	0.235	0.078	

Q=70 RE=.763E+07										
AOA	CN	CA	CCN	CCA	IL	LD	CL	CD	REDA	
8	52	98	54	100	43	74	0.064	0.251	0.126	
6	31	90	31	91	23	63	0.020	0.233	0.027	
4	11	71	12	71	8	54	0.010	0.137	0.028	
2	-7	56	-6	56	-8	47	-0.010	0.162	0.067	
0	-24	40	-23	39	-23	39	-0.033	0.134	0.056	
-2	-43	25	-42	25	-41	35	-0.053	0.120	0.050	
-4	-60	13	-59	19	-59	40	-0.074	0.133	0.053	
-6	-80	-4	-81	-9	-83	25	-0.103	0.087	0.036	
-8	-104	-39	-103	-44	-106	5	-0.136	0.019	0.007	
-10	-127	-45	-126	-54	-130	12	-0.167	0.040	0.017	

AOA	ANGLE OF ATTACK
CN	RAW NORMAL COUNTS
CA	RAW AXIAL COUNTS
CCN	CN CORRECTED FOR BALANCE INTERACTION
CCA	CA CORRECTED FOR BALANCE INTERACTION
IL	COUNTS OF LIFT
LD	COUNTS OF DRAG
CL	COEFFICIENT OF LIFT
CD	COEFFICIENT OF DRAG
RE	REYNOLDS NUMBER
Q	DYNAMIC PRESSURE, Q, IN POUNDS PER SQUARE FOOT
REDA	EQUIVALENT FLAT PLATE AREA (SQ FT)

Figure A.11 Data Output Files

NOSE/TAIL COMBINATION 2 (ATTACK/SYMMETRIC)									
WEIGHT = 22.3 LBS									
O=10 RE=.175E+07									
AOA	CN	CA	CCN	CCA	IT	TD	CL	CD	ERRA
8	9	41	9	40	6	5	0.153	0.220	0.191
6	6	29	6	29	4	5	0.133	0.136	0.056
4	3	23	1	22	0	7	-0.100	0.171	0.071
2	-1	14	0	14	0	6	-0.100	0.145	0.060
0	-3	6	-2	6	-2	6	-0.112	0.144	0.163
-2	-4	0	-3	1	-3	0	-0.125	0.217	0.091
-4	-5	-7	-4	-6	-4	10	-0.135	0.245	0.102
-6	-8	-19	-7	-12	-7	7	-0.163	0.160	0.067
-8	-9	-26	-8	-25	-8	8	-0.133	0.194	0.081
-10	-12	-34	-11	-33	-13	9	-0.118	0.216	0.090
O=30 RE=.303E+07									
AOA	CN	CA	CCN	CCA	IT	TD	CL	CD	ERRA
8	21	55	22	56	16	27	0.080	0.214	0.089
6	11	40	11	51	7	28	0.121	0.224	0.093
4	6	40	6	30	4	23	0.111	0.197	0.073
2	0	30	1	30	0	22	0.100	0.177	0.074
0	-3	20	-7	30	-7	20	-0.121	0.160	0.067
-2	-14	13	-13	13	-12	21	-0.127	0.171	0.071
-4	-20	6	-19	8	-17	23	-0.151	0.185	0.077
-6	-26	-5	-24	-14	-23	22	-0.163	0.172	0.075
-8	-35	-12	-34	-12	-33	25	-0.120	0.127	0.032
-10	-48	-29	-47	-31	-48	17	-0.145	0.138	0.057
O=50 RE=.301E+07									
AOA	CN	CA	CCN	CCA	IT	TD	CL	CD	ERRA
8	34	79	35	80	26	52	0.046	0.251	0.105
6	21	73	23	74	16	52	0.020	0.250	0.104
4	8	63	8	63	4	48	0.107	0.229	0.095
2	0	55	1	55	-1	48	-0.101	0.231	0.096
0	-12	40	-11	40	-11	40	-0.120	0.235	0.098
-2	-21	43	-20	43	-19	52	-0.133	0.243	0.103
-4	-33	35	-32	35	-29	53	-0.150	0.255	0.106
-6	-46	20	-45	30	-43	50	-0.122	0.200	0.121
-8	-50	12	-60	15	-55	56	-0.128	0.264	0.111
-10	-77	0	-76	4	-71	57	-0.127	0.272	0.113
O=70 RE=.463E+07									
AOA	CN	CA	CCN	CCA	IT	TD	CL	CD	ERRA
8	50	99	52	103	30	78	0.051	0.266	0.111
6	30	80	32	82	25	61	0.132	0.200	0.097
4	15	70	17	71	13	56	0.116	0.192	0.080
2	1	54	1	55	-1	47	-0.111	0.161	0.067
0	-16	45	-16	45	-16	46	-0.121	0.152	0.066
-2	-31	25	-30	25	-29	34	-0.137	0.117	0.043
-4	-45	15	-45	16	-43	35	-0.156	0.120	0.050
-6	-65	6	-65	11	-62	42	-0.120	0.142	0.052
-8	-82	-16	-82	-20	-83	25	-0.113	0.135	0.035
-10	-115	-37	-114	-45	-117	16	-0.150	0.152	0.022

AOA ANGLE OF ATTACK
 CN RAW NORMAL COUNTS
 CA RAW AXIAL COUNTS
 CCN CN CORRECTED FOR BALANCE INTERACTION
 CCA CA CORRECTED FOR BALANCE INTERACTION
 IT COUNTS OF LEFT
 TD COUNTS OF DRAG
 CL COEFFICIENT OF LIFT
 CD COEFFICIENT OF DRAG
 RE REYNOLDS NUMBER
 Q DYNAMIC PRESSURE, Q, IN POUNDS PER SQUARE FOOT
 ERRA EQUIVALENT FLAT PLATE AREA (SQ FT)

Figure A.11 Data Output Files(cont'd)

NOSE/TAIL COMBINATION 3 (ATTACK/LOW)										
REFRESH = 24.7 LBS										
O=10 PF=.175E+07										
AOA	CN	CA	CCN	CCA	TL	TD	CL	CD	PFPA	
0	11	42	11	41	3	3	0.063	0.186	0.078	
5	7	35	7	30	5	5	0.047	0.114	0.048	
10	4	22	4	22	3	3	0.023	0.120	0.050	
15	0	0	1	9	1	1	0.008	-0.014	-0.016	
20	-2	-2	-1	-2	-1	-1	-0.009	-0.048	-0.020	
25	-4	-7	-3	-5	-3	-3	-0.022	-0.065	-0.027	
30	-6	-15	-5	-14	-5	-4	-0.043	0.087	0.036	
35	-7	-27	-6	-26	-7	-1	-0.066	0.114	0.036	
40	-9	-38	-8	-37	-11	-1	-0.096	-0.028	-0.012	
45	-11	-48	-10	-47	-14	-2	-0.128	-0.041	-0.017	
O=30 PF=.301E+07										
AOA	CN	CA	CCN	CCA	TL	TD	CL	CD	PFPA	
0	30	55	30	57	24	25	0.173	0.210	0.088	
5	22	42	23	50	10	25	0.057	0.211	0.038	
10	13	38	13	37	11	21	0.033	0.165	0.062	
15	5	27	5	27	4	19	0.013	0.143	0.062	
20	-1	14	0	14	0	14	0.0	0.112	0.147	
25	-6	6	-8	6	-3	15	-0.023	0.119	0.050	
30	-15	2	-14	2	-13	20	-0.040	0.162	0.067	
35	-21	-13	-20	-12	-20	16	-0.059	0.123	0.053	
40	-32	-28	-31	-27	-32	12	-0.096	0.086	0.140	
45	-38	-40	-37	-40	-40	10	-0.119	0.079	0.033	
O=50 PF=.301E+07										
AOA	CN	CA	CCN	CCA	TL	TD	CL	CD	PFPA	
0	50	82	50	85	40	57	0.173	0.272	0.114	
5	36	73	37	75	30	53	0.055	0.253	0.105	
10	20	62	21	63	17	47	0.031	0.226	0.094	
15	3	46	9	47	7	39	0.012	0.185	0.077	
20	-2	36	-1	35	-1	35	-0.002	0.163	0.070	
25	-14	30	-13	30	-12	39	-0.021	0.137	0.078	
30	-27	20	-26	20	-24	30	-0.043	0.137	0.073	
35	-39	13	-37	14	-34	44	-0.061	0.209	0.097	
40	-58	-3	-53	-3	-50	39	-0.091	0.136	0.078	
45	-68	-15	-68	-17	-66	33	-0.119	0.182	0.076	
O=70 PF=.463E+07										
AOA	CN	CA	CCN	CCA	TL	TD	CL	CD	PFPA	
0	71	90	73	104	61	79	0.077	0.270	0.113	
5	51	80	52	93	43	72	0.056	0.247	0.103	
10	29	75	31	77	25	62	0.034	0.212	0.088	
15	10	60	10	60	9	52	0.010	0.179	0.074	
20	-3	40	-7	40	-7	40	-0.009	0.137	0.057	
25	-23	27	-22	27	-21	36	-0.027	0.125	0.052	
30	-45	10	-43	12	-41	30	-0.053	0.110	0.046	
35	-60	-9	-58	-11	-57	21	-0.074	0.072	0.030	
40	-82	-30	-81	-32	-82	13	-0.106	0.044	0.019	
45	-104	-50	-103	-56	-107	6	-0.138	0.019	0.003	
AOA	ANGLE OF ATTACK									
CN	RAW NORMAL COUNTS									
CA	RAW AXIAL COUNTS									
CCN	CN CORRECTED FOR BALANCE INTERACTION									
CCA	CA CORRECTED FOR BALANCE INTERACTION									
TL	COUNTS OF LIFT									
TD	COUNTS OF DRAG									
CL	COEFFICIENT OF LIFT									
CD	COEFFICIENT OF DRAG									
PF	REYNOLDS NUMBER									
O	DYNAMIC PRESSURE, Q, IN POUNDS PER SQUARE FOOT									
PFPA	EQUIVALENT FLAT PLATE AREA (SQ FT)									

Figure A.11 Data Output Files(cont'd)

NOSE/TAIL COMBINATION 4 (BLUNT/RIGHT)

HEIGHT = 23.2183
 Q=10 PF=.175E+17

AOA	CN	CA	CCN	CCA	IL	ID	CI	CJ	REF
0	30	40	30	30	5	7	0.043	0.177	0.074
6	3	20	3	20	1	5	0.011	0.117	0.040
4	0	23	1	23	0	7	0.000	0.163	0.063
2	-2	10	-1	10	-1	2	0.011	0.044	0.013
0	-4	7	-3	7	-3	7	0.027	0.163	0.070
-2	-8	-4	-7	-3	-7	5	0.063	0.129	0.054
-4	-10	-10	-9	-3	-9	9	0.091	0.189	0.079
-6	-12	-13	-11	-17	-11	9	0.103	0.205	0.085
-8	-15	-20	-18	-23	-15	7	0.139	0.167	0.066
-10	-17	-36	-16	-34	-13	10	0.163	0.231	0.096

Q=30 PF=.303E+17

AOA	CN	CA	CCN	CCA	IL	ID	CI	CJ	REF
0	30	55	30	57	24	28	0.072	0.226	0.094
6	20	55	21	52	17	30	0.055	0.237	0.090
4	12	40	12	30	10	24	0.020	0.183	0.073
2	4	33	4	33	3	25	0.000	0.200	0.033
0	-4	22	-3	22	-3	22	0.000	0.176	0.073
-2	-12	14	-11	14	-10	22	0.031	0.130	0.075
-4	-18	4	-17	4	-16	21	0.043	0.171	0.071
-6	-23	-6	-27	-5	-26	23	0.073	0.177	0.071
-8	-34	-15	-33	-14	-32	23	0.097	0.185	0.077
-10	-43	-25	-41	-24	-41	24	0.123	0.191	0.079

Q=50 PF=.391E+17

AOA	CN	CA	CCN	CCA	IL	ID	CI	CJ	REF
0	48	80	48	91	37	64	0.067	0.302	0.123
6	32	70	34	81	27	60	0.043	0.237	0.120
4	18	70	21	71	17	56	0.030	0.253	0.112
2	6	65	7	65	5	57	0.000	0.274	0.114
0	-6	57	-4	57	-4	57	0.007	0.274	0.114
-2	-20	41	-19	40	-17	40	0.011	0.234	0.097
-4	-32	30	-31	30	-28	40	0.051	0.232	0.097
-6	-45	22	-43	22	-30	52	0.070	0.243	0.103
-8	-50	13	-58	15	-53	55	0.096	0.265	0.111
-10	-48	0	-74	3	-60	56	0.124	0.270	0.112

Q=70 PF=.463E+17

AOA	CN	CA	CCN	CCA	IL	ID	CI	CJ	REF
0	65	110	67	114	53	90	0.063	0.302	0.123
6	43	100	44	103	34	83	0.044	0.291	0.119
4	22	90	23	95	17	80	0.022	0.275	0.115
2	6	77	7	73	5	65	0.006	0.223	0.093
0	-6	62	-7	62	-7	62	0.000	0.213	0.080
-2	-30	40	-29	40	-27	43	0.015	0.163	0.070
-4	-40	33	-48	24	-46	42	0.050	0.148	0.060
-6	-50	17	-53	14	-65	45	0.083	0.155	0.065
-8	-50	0	-60	6	-84	51	0.108	0.173	0.070
-10	-108	-15	-107	-20	-105	39	0.135	0.135	0.056

AOA ANGLE OF ATTACK
 CN RAW NOSE/TAI COUNTS
 CA RAW AYTAL COUNTS
 CCN CN CORRECTED FOR BALANCE INTERACTION
 CCA CA CORRECTED FOR BALANCE INTERACTION
 IL COUNTS OF LIST
 ID COUNTS OF DBA
 CI COEFFICIENT OF LIST
 CJ COEFFICIENT OF DBA
 PF DYNAMIC PRESSURE, Q, IN POUNDS PER SQUARE FOOT
 Q REFRA EQUIVALENT FLAT PLATE AREA (SQ FT)

Figure A.11 Data Output Files(cont'd)

NOSE/TAIL COMBINATION 5 (BLUNT/SYMMETRIC)										
WEIGHT = 21.3 LBS										
Q=10 BF=.175E+07										
AOA	CH	CA	CCW	CCA	IL	ID	CI	CD	CDPA	BEPA
0	0	0	0	0	0	0	0	0.000	0.041	
5	4	28	4	28	0	0	0.000	0.143	0.060	
10	1	22	1	22	0	0	0.000	0.171	0.071	
15	-1	13	0	13	0	0	0.000	0.133	0.055	
20	-2	5	-1	5	-1	5	-0.000	0.120	0.050	
25	-4	-3	-3	-3	-3	5	-0.000	0.133	0.056	
30	-7	-10	-5	-10	-5	7	-0.000	0.176	0.073	
35	-10	-22	-10	-22	-10	10	-0.000	0.251	0.121	
40	-11	-37	-10	-36	-11	20	-0.000	0.053	0.022	
45	-11	-37	-10	-36	-11	20	-0.000	0.090	0.033	

Q=30 BF=.303E+07										
AOA	CH	CA	CCW	CCA	IL	ID	CI	CD	CDPA	BEPA
0	0	0	0	0	0	0	0	0.274	0.114	
5	15	40	17	50	12	30	0.000	0.234	0.087	
10	0	40	9	30	7	25	0.000	0.197	0.080	
15	-3	30	3	30	-2	23	-0.000	0.191	0.075	
20	-10	21	-12	21	-3	21	-0.000	0.163	0.070	
25	-17	13	-18	13	-13	21	-0.000	0.165	0.060	
30	-25	0	-15	1	-14	17	-0.000	0.135	0.056	
35	-32	-10	-24	-10	-24	16	-0.000	0.127	0.053	
40	-40	-34	-38	-33	-40	11	-0.000	0.089	0.037	
45	-40	-34	-38	-33	-40	11	-0.000	0.089	0.037	

Q=50 BF=.301E+07										
AOA	CH	CA	CCW	CCA	IL	ID	CI	CD	CDPA	BEPA
0	0	0	0	0	0	0	0	0.317	0.132	
5	29	78	31	80	24	51	0.000	0.290	0.121	
10	13	57	20	63	16	54	0.000	0.261	0.100	
15	-6	58	6	58	4	51	0.000	0.243	0.101	
20	-15	45	-1	45	-1	46	-0.000	0.221	0.080	
25	-29	36	-14	35	-13	43	-0.000	0.206	0.086	
30	-40	2	-38	2	-35	35	-0.000	0.167	0.060	
35	-53	-15	-52	-6	-50	31	-0.000	0.140	0.050	
40	-60	-22	-60	-24	-63	25	-0.000	0.121	0.050	
45	-60	-22	-60	-24	-63	25	-0.000	0.121	0.050	

Q=70 BF=.463E+07										
AOA	CH	CA	CCW	CCA	IL	ID	CI	CD	CDPA	BEPA
0	0	0	0	0	0	0	0	0.360	0.151	
5	48	100	45	111	34	80	0.000	0.313	0.133	
10	27	86	29	98	22	85	0.000	0.291	0.121	
15	10	75	11	75	9	83	0.000	0.273	0.107	
20	-3	63	-2	63	-2	80	-0.000	0.273	0.099	
25	-21	40	-20	39	-13	77	-0.000	0.150	0.067	
30	-40	20	-40	20	-33	78	-0.000	0.120	0.054	
35	-61	0	-61	1	-59	70	-0.000	0.102	0.040	
40	-73	-4	-77	-3	-75	71	-0.000	0.108	0.045	
45	-101	-20	-100	-25	-100	30	-0.000	0.102	0.040	

AOA ANGLE OF ATTACK
 CH 2ND NORMAL COUNTS
 CA 2ND AXIAL COUNTS
 CCW CH CORRECTED FOR BALANCE INTERACTION
 CCA CA CORRECTED FOR BALANCE INTERACTION
 IL COUNTS OF LIFT
 ID COUNTS OF DRAG
 CI COEFFICIENT OF LIFT
 CD COEFFICIENT OF DRAG
 BF STAYING MOMENT
 Q DYNAMIC PRESSURE IN POUNDS PER SQUARE FOOT
 BEPA EQUIVALENT PLATE AREA (SQ FT)

Figure A.11 Data Output Files(cont'd)

NOSF/TAIL COMBINATION 6 (BLUNT/LOW)

WEIGHT = 33.2 LBS
 $\alpha = 10^\circ$ $Re = .175E+07$

AOA	CM	CA	CCM	CCA	IL	ID	CL	CD	SPRA
8	11	47	11	49	6	13	0.057	0.425	0.177
6	7	40	7	39	4	15	0.037	0.355	0.152
4	4	30	4	30	2	14	0.022	0.335	0.140
2	1	22	1	22	0	14	0.003	0.334	0.130
0	-1	15	0	15	0	15	0.0	0.360	0.150
-2	-3	5	-2	5	-2	13	-0.015	0.316	0.132
-4	-5	0	-4	1	-3	17	-0.030	0.420	0.175
-6	-7	-5	-6	-4	-5	21	-0.045	0.503	0.200
-8	-8	-13	-7	-17	-7	16	-0.063	0.395	0.165
-10	-9	-25	-8	-24	-7	12	-0.077	0.434	0.131

$\alpha = 30^\circ$ $Re = .303E+07$

AOA	CM	CA	CCM	CCA	IL	ID	CL	CD	SPRA
8	36	56	36	53	30	30	0.000	0.241	0.100
6	24	48	25	50	21	39	0.063	0.224	0.094
4	17	40	17	40	15	35	0.044	0.199	0.083
2	10	30	10	30	0	32	0.027	0.173	0.074
0	2	21	2	21	2	31	0.006	0.153	0.070
-2	-6	12	-5	12	-4	20	-0.013	0.162	0.063
-4	-13	3	-12	3	-11	20	-0.034	0.150	0.067
-6	-20	-3	-19	-2	-17	24	-0.051	0.133	0.061
-8	-30	-17	-23	-16	-23	20	-0.083	0.163	0.068
-10	-37	-25	-35	-24	-35	23	-0.105	0.182	0.076

$\alpha = 50^\circ$ $Re = .301E+07$

AOA	CM	CA	CCM	CCA	IL	ID	CL	CD	SPRA
8	60	85	61	82	50	63	0.001	0.304	0.127
6	47	75	47	70	40	50	0.072	0.284	0.113
4	35	65	35	63	31	54	0.055	0.260	0.109
2	20	56	21	57	10	50	0.034	0.238	0.090
0	6	47	6	40	6	40	0.011	0.235	0.088
-2	-3	38	-2	37	-1	45	-0.001	0.217	0.080
-4	-17	30	-16	30	-13	47	-0.024	0.227	0.085
-6	-30	20	-29	20	-25	47	-0.046	0.227	0.084
-8	-45	9	-42	11	-39	49	-0.070	0.236	0.088
-10	-53	0	-52	1	-48	50	-0.086	0.242	0.101

$\alpha = 70^\circ$ $Re = .463E+07$

AOA	CM	CA	CCM	CCA	IL	ID	CL	CD	SPRA
8	37	84	30	101	76	80	0.008	0.275	0.114
6	63	84	60	38	61	70	0.072	0.242	0.101
4	40	70	50	74	45	61	0.053	0.200	0.087
2	29	50	29	60	26	53	0.033	0.181	0.075
0	5	40	5	30	5	30	0.006	0.134	0.056
-2	-12	20	-11	20	-11	23	-0.013	0.093	0.041
-4	-30	3	-28	3	-27	21	-0.035	0.073	0.030
-6	-50	-10	-49	-11	-40	13	-0.062	0.163	0.026
-8	-63	-23	-68	-26	-60	17	-0.083	0.058	0.024
-10	-92	-45	-93	-51	-97	6	-0.125	0.022	0.009

AOA ANGLE OF ATTACK
 CM PAN NORMAL COUNTS
 CA PAN AXIAL COUNTS
 CCM CM CORRECTED FOR BALANCE INTERACTION
 CCA CA CORRECTED FOR BALANCE INTERACTION
 IL COUNTS OF LEFT
 ID COUNTS OF RIGHT
 CL COEFFICIENT OF LIFT
 CD COEFFICIENT OF DRAG
 Re DYNAMIC PRESSURE
 SPRA DYNAMIC PRESSURE CO. IN POUNDS PER SQUARE FOOT
 EQUIVALENT FLAT PLATE AREA (SQ FT)

Figure A.11 Data Output Files(cont'd)

WOSP/TAIL COMBINATION 7 (SMOOTH/HIGH)

HEIGHT = 22.7 IN
Q = 10 PS = .1757E+07

AOA	CN	CA	CCN	CCA	TL	TD	CL	CD	EFFA
8	8	40	3	38	2	10	0.042	0.185	0.031
6	4	34	4	34	2	10	0.015	0.252	0.135
4	1	26	1	26	0	10	-0.002	0.244	0.122
2	-3	20	-1	20	-3	12	-0.014	0.283	0.123
0	-6	7	-5	7	-5	7	-0.045	0.163	0.070
-2	-9	2	-3	2	-3	10	-0.073	0.245	0.122
-4	-10	-4	-3	-3	-3	13	-0.078	0.324	0.135
-6	-13	-18	-12	-17	-12	9	-0.112	0.194	0.031
-8	-16	-23	-14	-22	-15	12	-0.132	0.233	0.113
-10	-19	-32	-17	-31	-19	12	-0.163	0.295	0.119

Q = 30 PS = .3035E+07

AOA	CN	CA	CCN	CCA	TL	TD	CL	CD	EFFA
8	15	44	16	45	12	15	0.035	0.121	0.051
6	3	32	8	33	6	10	0.017	0.370	0.033
4	1	28	1	29	0	12	-0.011	0.097	0.041
2	-3	12	-1	13	-1	10	-0.024	0.030	0.032
0	-6	7	-7	7	-7	7	-0.021	0.056	0.022
-2	-15	-3	-14	-3	-14	6	-0.042	0.051	0.021
-4	-19	-12	-18	-11	-18	6	-0.055	0.043	0.020
-6	-25	-22	-23	-21	-24	5	-0.071	0.042	0.018
-8	-30	-35	-32	-31	-31	4	-0.093	0.032	0.013
-10	-37	-43	-36	-45	-40	1	-0.110	0.011	0.005

Q = 50 PS = .5015E+07

AOA	CN	CA	CCN	CCA	TL	TD	CL	CD	EFFA
8	42	92	42	94	31	67	0.055	0.323	0.135
6	27	79	29	80	22	59	0.039	0.292	0.113
4	13	70	14	70	10	55	0.017	0.264	0.110
2	1	63	1	63	-1	55	-0.002	0.268	0.110
0	-13	45	-12	45	-12	45	-0.022	0.216	0.090
-2	-26	35	-25	35	-24	44	-0.043	0.210	0.083
-4	-41	17	-39	13	-37	37	-0.067	0.175	0.073
-6	-56	3	-55	5	-53	35	-0.095	0.170	0.071
-8	-70	-8	-69	-11	-68	30	-0.122	0.146	0.061
-10	-92	-20	-91	-23	-90	31	-0.145	0.148	0.062

Q = 70 PS = .4635E+07

AOA	CN	CA	CCN	CCA	TL	TD	CL	CD	EFFA
8	65	114	68	119	53	95	0.068	0.325	0.135
6	39	90	39	91	31	71	0.039	0.243	0.101
4	20	80	22	81	17	66	0.022	0.223	0.095
2	0	53	1	53	-1	50	-0.001	0.172	0.072
0	-20	45	-20	46	-20	46	-0.026	0.153	0.066
-2	-40	25	-39	25	-38	34	-0.049	0.118	0.049
-4	-62	5	-62	3	-62	29	-0.073	0.100	0.042
-6	-84	-12	-83	-16	-83	17	-0.107	0.057	0.024
-8	-105	-20	-104	-25	-104	20	-0.134	0.070	0.023
-10	-128	-37	-127	-46	-130	16	-0.167	0.056	0.023

AOA ANGLE OF ATTACK
CN RAW NORMAL COUNTS
CA RAW AXIAL COUNTS
CCN CN CORRECTED FOR BALANCE INTERACTION
CCA CA CORRECTED FOR BALANCE INTERACTION
TL COUNTS OF LEFT
TD COUNTS OF RIGHT
CL COEFFICIENT OF LIFT
CD COEFFICIENT OF DRAG
PS DYNAMIC PRESSURE, O. IN POUNDS PER SQUARE FOOT
Q DYNAMIC PRESSURE, O. IN POUNDS PER SQUARE FOOT
EFFA EQUIVALENT FLAT PLATE AREA (SQ FT)

Figure A.11 Data Output Files(cont'd)

NOSE/TAIL COMBINATION 8 (SMOOTH/SYMMETRIC)
 REYNOLDS NUMBER = 20,000,000
 PRANDTL NUMBER = 0.75
 DENSITY = 1.75E+07

AOA	CN	CA	CCN	CCA	IL	TD	CL	CD	REFDA
0	0	0	0	0	0	0	0.000	0.000	0.000
2	0	0	0	0	0	0	0.000	0.000	0.000
4	0	0	0	0	0	0	0.000	0.000	0.000
6	0	0	0	0	0	0	0.000	0.000	0.000
8	0	0	0	0	0	0	0.000	0.000	0.000
10	0	0	0	0	0	0	0.000	0.000	0.000
12	0	0	0	0	0	0	0.000	0.000	0.000
14	0	0	0	0	0	0	0.000	0.000	0.000
16	0	0	0	0	0	0	0.000	0.000	0.000
18	0	0	0	0	0	0	0.000	0.000	0.000
20	0	0	0	0	0	0	0.000	0.000	0.000
22	0	0	0	0	0	0	0.000	0.000	0.000
24	0	0	0	0	0	0	0.000	0.000	0.000
26	0	0	0	0	0	0	0.000	0.000	0.000
28	0	0	0	0	0	0	0.000	0.000	0.000
30	0	0	0	0	0	0	0.000	0.000	0.000
32	0	0	0	0	0	0	0.000	0.000	0.000
34	0	0	0	0	0	0	0.000	0.000	0.000
36	0	0	0	0	0	0	0.000	0.000	0.000
38	0	0	0	0	0	0	0.000	0.000	0.000
40	0	0	0	0	0	0	0.000	0.000	0.000
42	0	0	0	0	0	0	0.000	0.000	0.000
44	0	0	0	0	0	0	0.000	0.000	0.000
46	0	0	0	0	0	0	0.000	0.000	0.000
48	0	0	0	0	0	0	0.000	0.000	0.000
50	0	0	0	0	0	0	0.000	0.000	0.000
52	0	0	0	0	0	0	0.000	0.000	0.000
54	0	0	0	0	0	0	0.000	0.000	0.000
56	0	0	0	0	0	0	0.000	0.000	0.000
58	0	0	0	0	0	0	0.000	0.000	0.000
60	0	0	0	0	0	0	0.000	0.000	0.000
62	0	0	0	0	0	0	0.000	0.000	0.000
64	0	0	0	0	0	0	0.000	0.000	0.000
66	0	0	0	0	0	0	0.000	0.000	0.000
68	0	0	0	0	0	0	0.000	0.000	0.000
70	0	0	0	0	0	0	0.000	0.000	0.000
72	0	0	0	0	0	0	0.000	0.000	0.000
74	0	0	0	0	0	0	0.000	0.000	0.000
76	0	0	0	0	0	0	0.000	0.000	0.000
78	0	0	0	0	0	0	0.000	0.000	0.000
80	0	0	0	0	0	0	0.000	0.000	0.000
82	0	0	0	0	0	0	0.000	0.000	0.000
84	0	0	0	0	0	0	0.000	0.000	0.000
86	0	0	0	0	0	0	0.000	0.000	0.000
88	0	0	0	0	0	0	0.000	0.000	0.000
90	0	0	0	0	0	0	0.000	0.000	0.000
92	0	0	0	0	0	0	0.000	0.000	0.000
94	0	0	0	0	0	0	0.000	0.000	0.000
96	0	0	0	0	0	0	0.000	0.000	0.000
98	0	0	0	0	0	0	0.000	0.000	0.000
100	0	0	0	0	0	0	0.000	0.000	0.000

ANGLE OF ATTACK
 CN NOSE/TAIL COUNTS
 CA NOSE/TAIL COUNTS
 CCN NOSE/TAIL COUNTS
 CCA NOSE/TAIL COUNTS
 IL NOSE/TAIL COUNTS
 TD NOSE/TAIL COUNTS
 CL NOSE/TAIL COUNTS
 CD NOSE/TAIL COUNTS
 REFDA NOSE/TAIL COUNTS
 DYNAMIC PRESSURE IN POUNDS PER SQUARE FOOT
 EQUIVALENT FLAT PLATE AREA (SQ FT)

Figure A.11 Data Output Files(cont'd)

NOSE/TAIL COMBINATION 0 (SMOOTH/LOZ)									
WEIGHT = 22.7 LBS									
Q=10 RE=.175E+07									
AOA	CN	CA	CCN	CCA	TL	TD	CL	CD	PPPA
8	12	42	12	41	8	11	0.075	0.256	0.107
6	9	28	9	28	7	6	0.054	0.145	0.060
4	5	20	5	20	4	4	0.037	0.107	0.045
2	3	7	2	7	2	-1	0.017	-0.021	0.020
0	0	2	1	2	1	2	0.002	0.043	0.020
-2	-2	-7	-1	-6	-1	2	-0.010	0.047	0.020
-4	-4	-19	-3	-13	-4	-2	-0.033	-0.046	-0.019
-6	-6	-34	-5	-23	-6	-1	-0.055	-0.034	-0.014
-8	-8	-48	-7	-37	-8	-1	-0.080	-0.100	-0.042
-10	-9	-45	-8	-44	-12	-2	-0.109	-0.060	-0.025

Q=30 RE=.303E+07									
AOA	CN	CA	CCN	CCA	TL	TD	CL	CD	PPPA
8	38	60	38	60	31	15	0.094	0.281	0.117
6	28	52	28	55	24	14	0.073	0.272	0.113
4	20	40	20	41	18	13	0.053	0.204	0.085
2	10	20	10	20	9	11	0.027	0.171	0.071
0	4	13	4	13	4	13	0.012	0.144	0.060
-2	-2	-13	-1	-12	-1	10	-0.002	0.080	0.033
-4	-13	-13	-11	-11	-11	6	-0.034	0.045	0.010
-6	-21	-22	-19	-21	-20	5	-0.060	0.030	0.015
-8	-30	-33	-29	-32	-31	4	-0.083	0.032	0.013
-10	-36	-47	-35	-50	-40	-4	-0.119	-0.030	-0.012

Q=50 RE=.391E+07									
AOA	CN	CA	CCN	CCA	TL	TD	CL	CD	PPPA
8	53	83	50	86	40	22	0.088	0.286	0.124
6	41	77	45	79	38	20	0.068	0.286	0.110
4	27	63	27	64	23	19	0.041	0.219	0.100
2	14	58	14	55	12	18	0.022	0.229	0.085
0	1	30	1	30	1	33	0.002	0.182	0.076
-2	-13	26	-12	26	-11	34	-0.000	0.165	0.059
-4	-29	18	-28	18	-26	36	-0.047	0.172	0.072
-6	-43	3	-41	4	-39	32	-0.070	0.154	0.064
-8	-57	-12	-55	-14	-54	25	-0.098	0.122	0.051
-10	-72	-28	-72	-31	-73	21	-0.131	0.103	0.043

Q=70 RE=.463E+07									
AOA	CN	CA	CCN	CCA	TL	TD	CL	CD	PPPA
8	83	108	87	115	72	24	0.093	0.324	0.135
6	62	90	62	92	54	25	0.070	0.253	0.102
4	40	80	41	82	36	26	0.045	0.236	0.088
2	19	64	20	55	18	28	0.023	0.164	0.069
0	0	35	1	35	1	35	0.001	0.120	0.050
-2	-21	20	-20	20	-12	30	-0.025	0.098	0.041
-4	-47	0	-40	1	-30	20	-0.051	0.067	0.039
-6	-64	-21	-64	-22	-65	0	-0.083	0.022	0.012
-8	-84	-42	-84	-43	-83	-1	-0.113	-0.014	-0.015
-10	-105	-65	-104	-71	-111	-12	-0.143	-0.043	-0.018

AOA ANGLE OF ATTACK
 CN RAY NORMAL COUNTS
 CA RAY AXIAL COUNTS
 CCN CN CORRECTED FOR BALANCE INTERACTION
 CCA CA CORRECTED FOR BALANCE INTERACTION
 TL COUNTS OF LIFT
 TD COUNTS OF DRAG
 CL COEFFICIENT OF LIFT
 CD COEFFICIENT OF DRAG
 RE DYNAMIC PRESSURE, Q, IN POUNDS PER SQUARE FOOT
 Q DYNAMIC PRESSURE, Q, IN POUNDS PER SQUARE FOOT
 PPPA EQUIVALENT FLAT PLATE AREA (SQ FT)

Figure A.11 Data Output Files(cont'd)

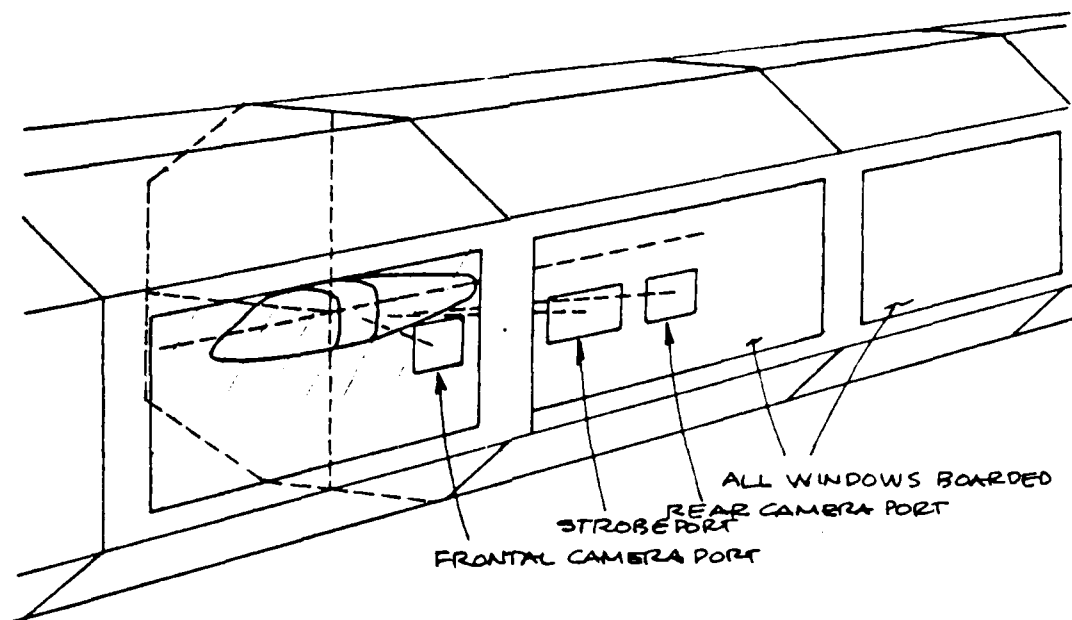


Figure A.12 Layout for Mini-tufting Photography

APPENDIX B GRAPHICAL RESULTS

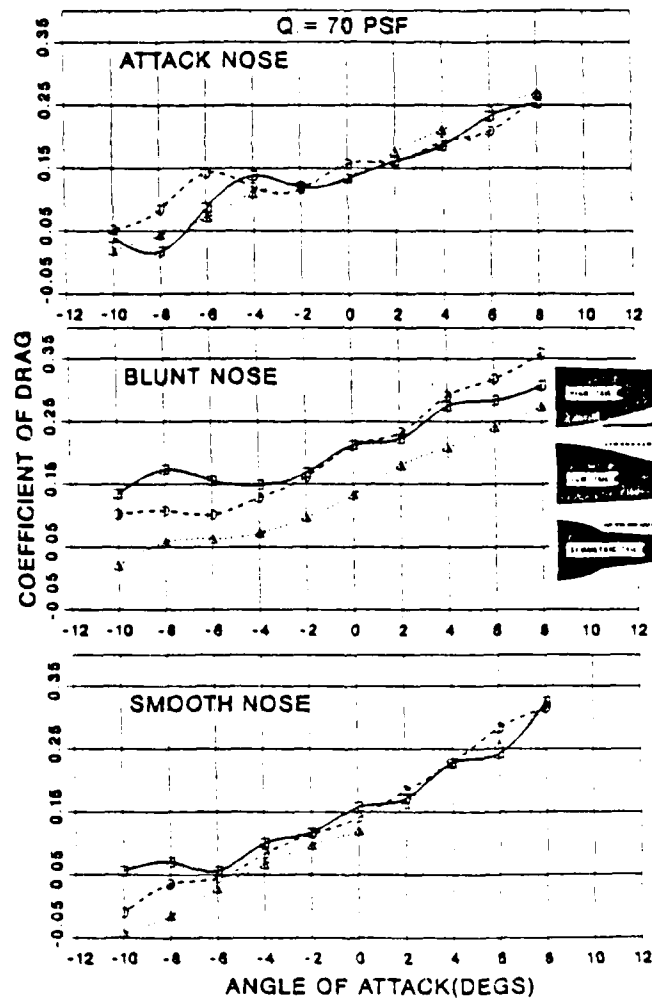


Figure B.1 Cd Versus AOA

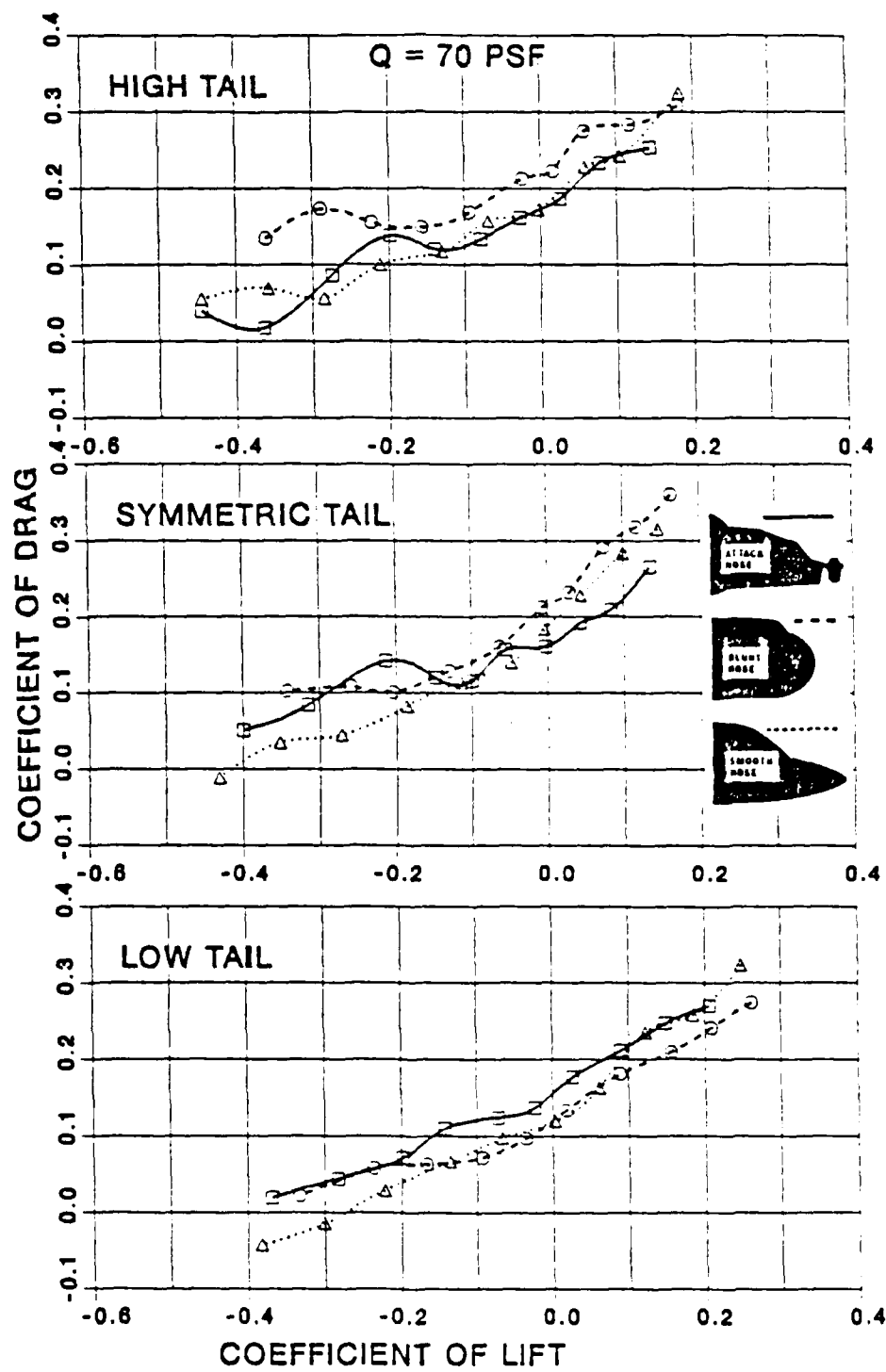


Figure B.2 C_d Versus C_l

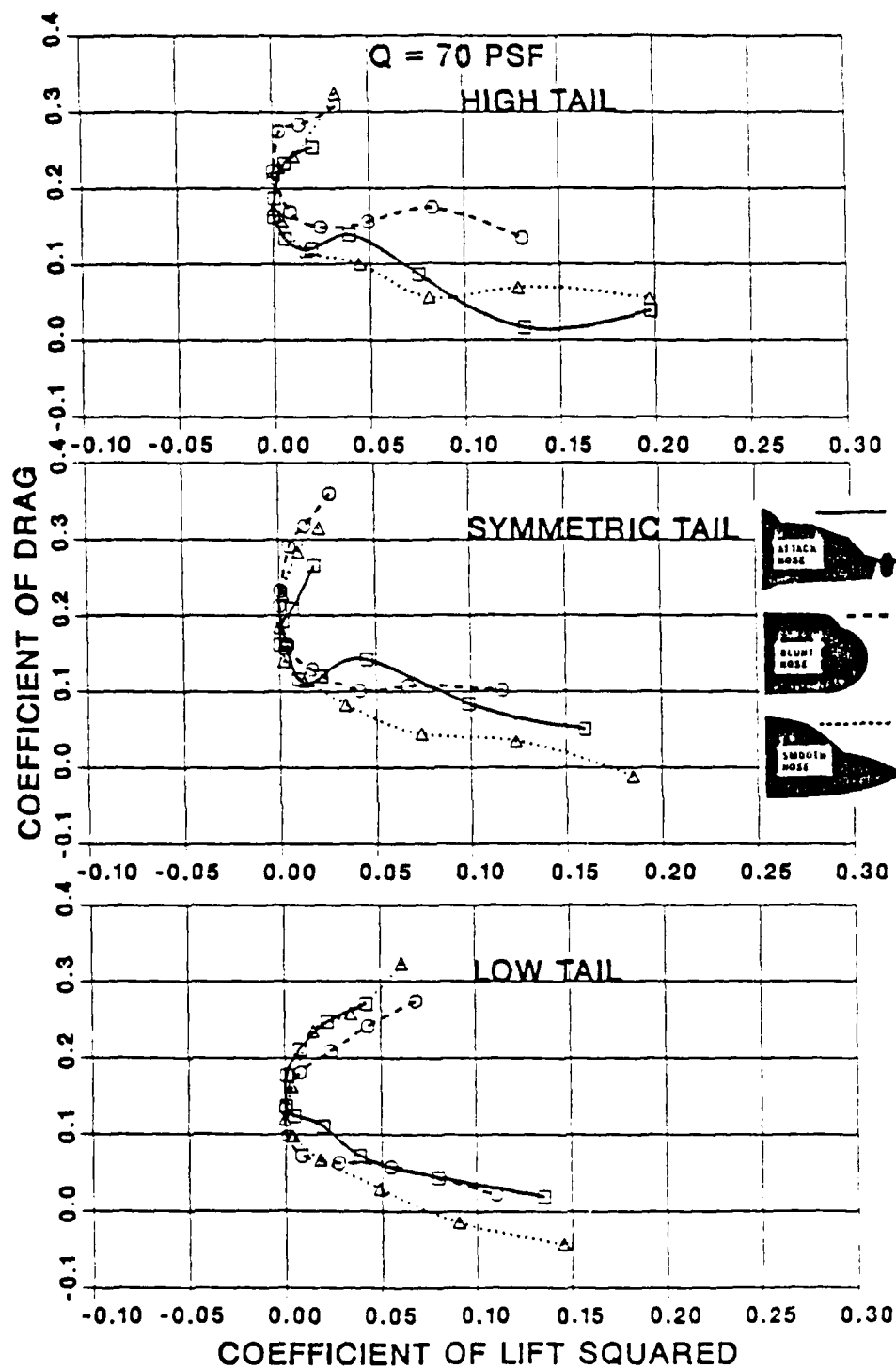


Figure B.3 Cd Versus Cl Squared

APPENDIX C
FLOW VISUALIZATION RESULTS

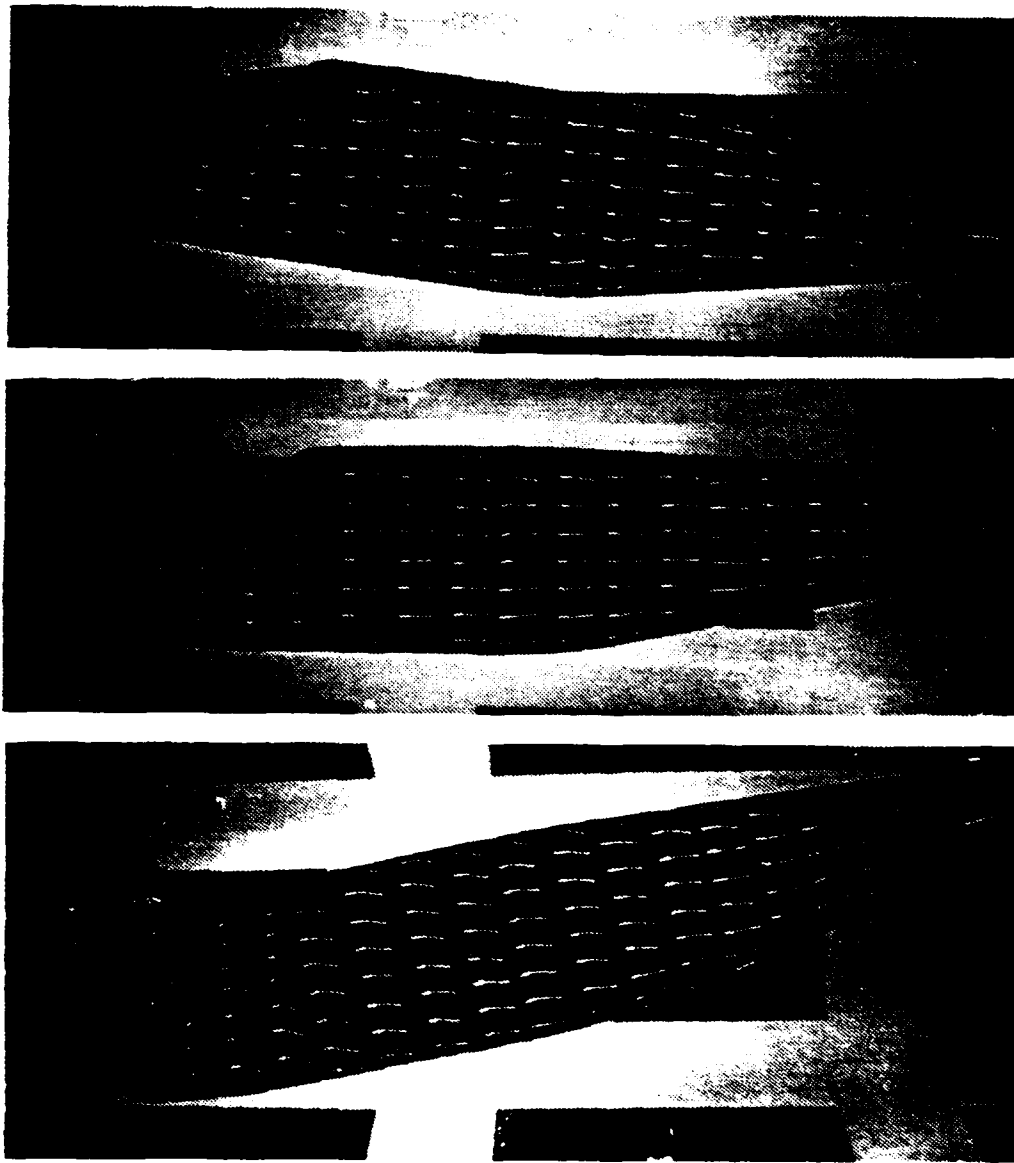


Figure C.1 Attack Nose/ High Tail

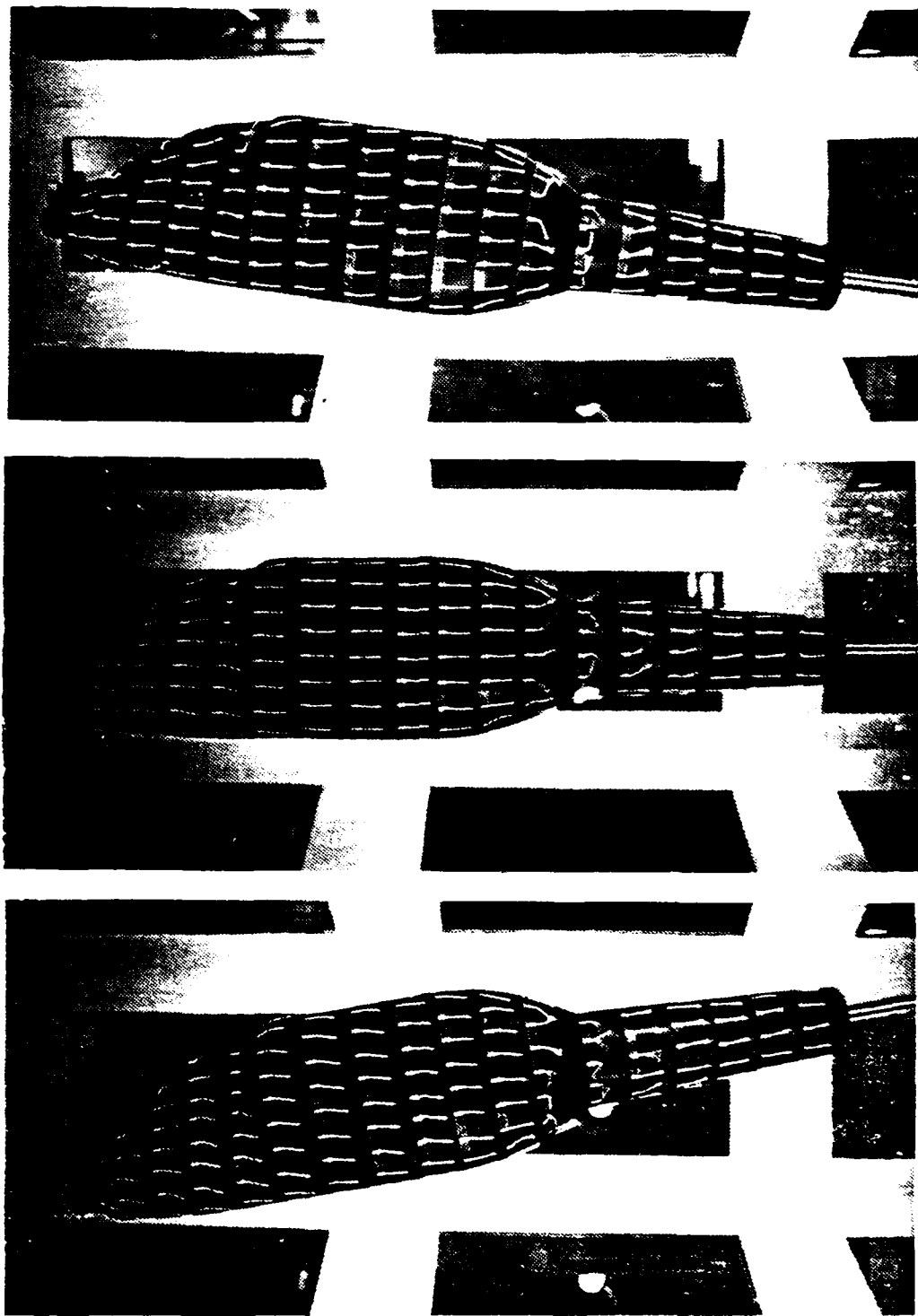


Figure C.2 Attack Nose/ Symmetric Tail

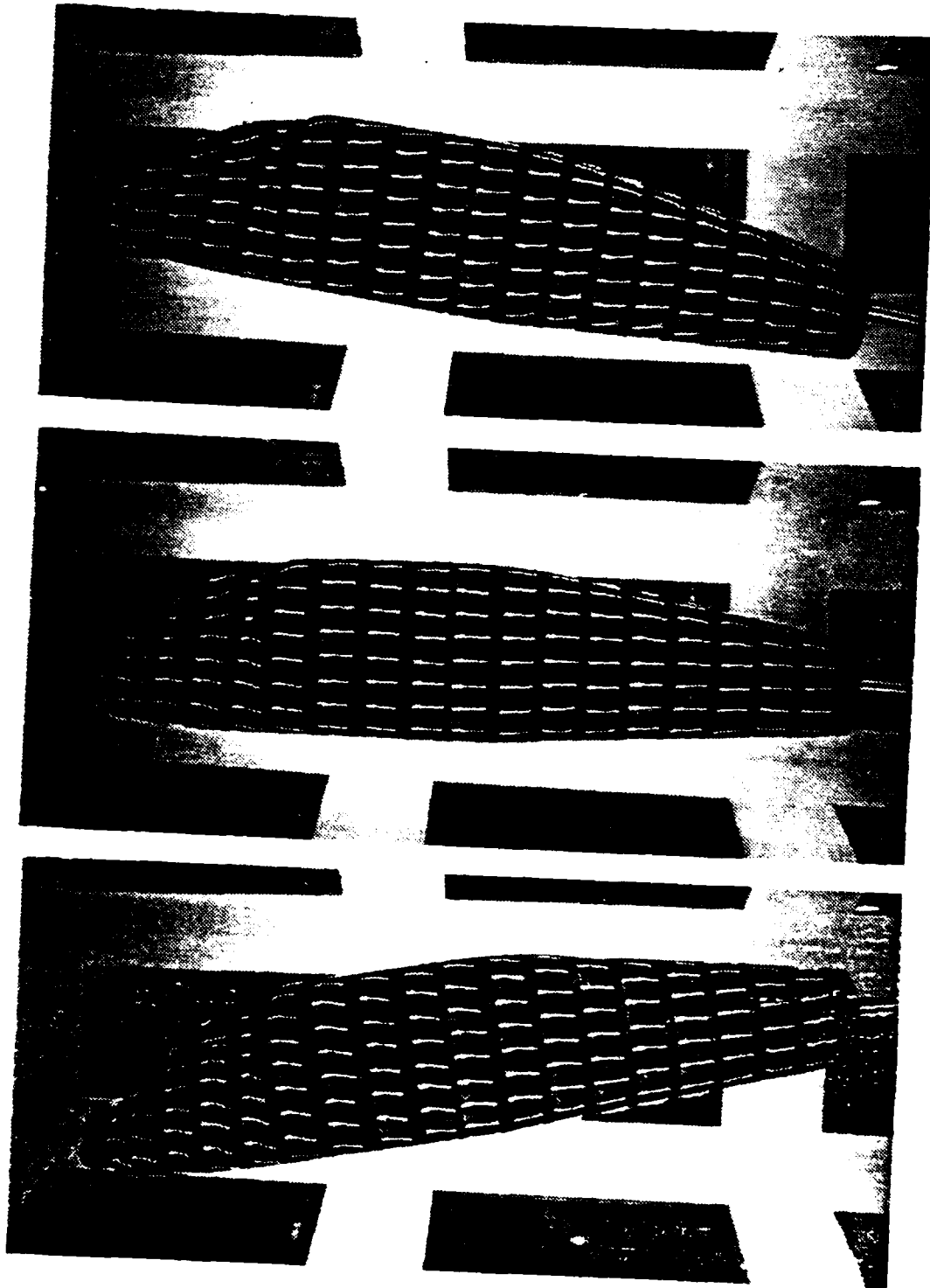


Figure C.3 Attack Nose Low Tail

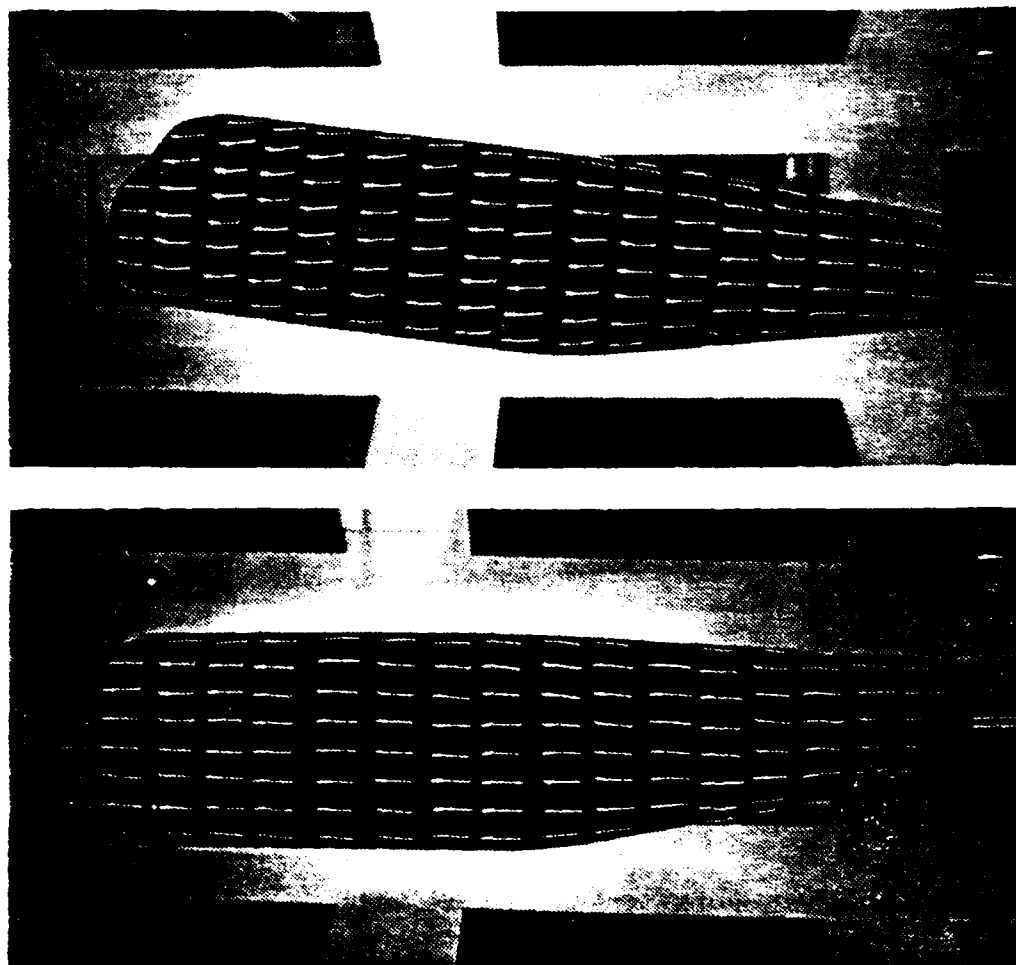


Figure C.1 Blunt Nose High Tail

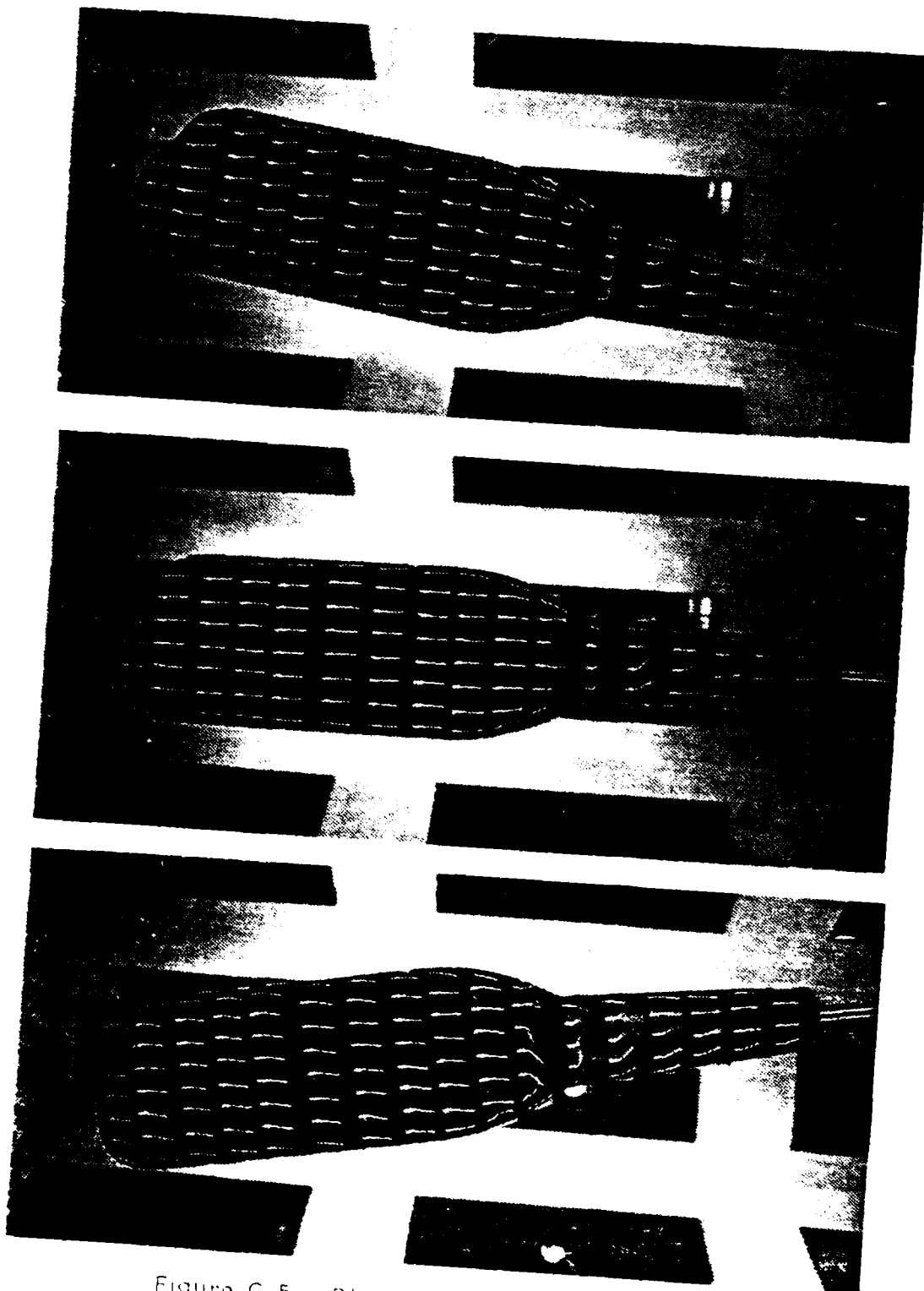


Figure C.5 Blunt Nose Symmetric Tail

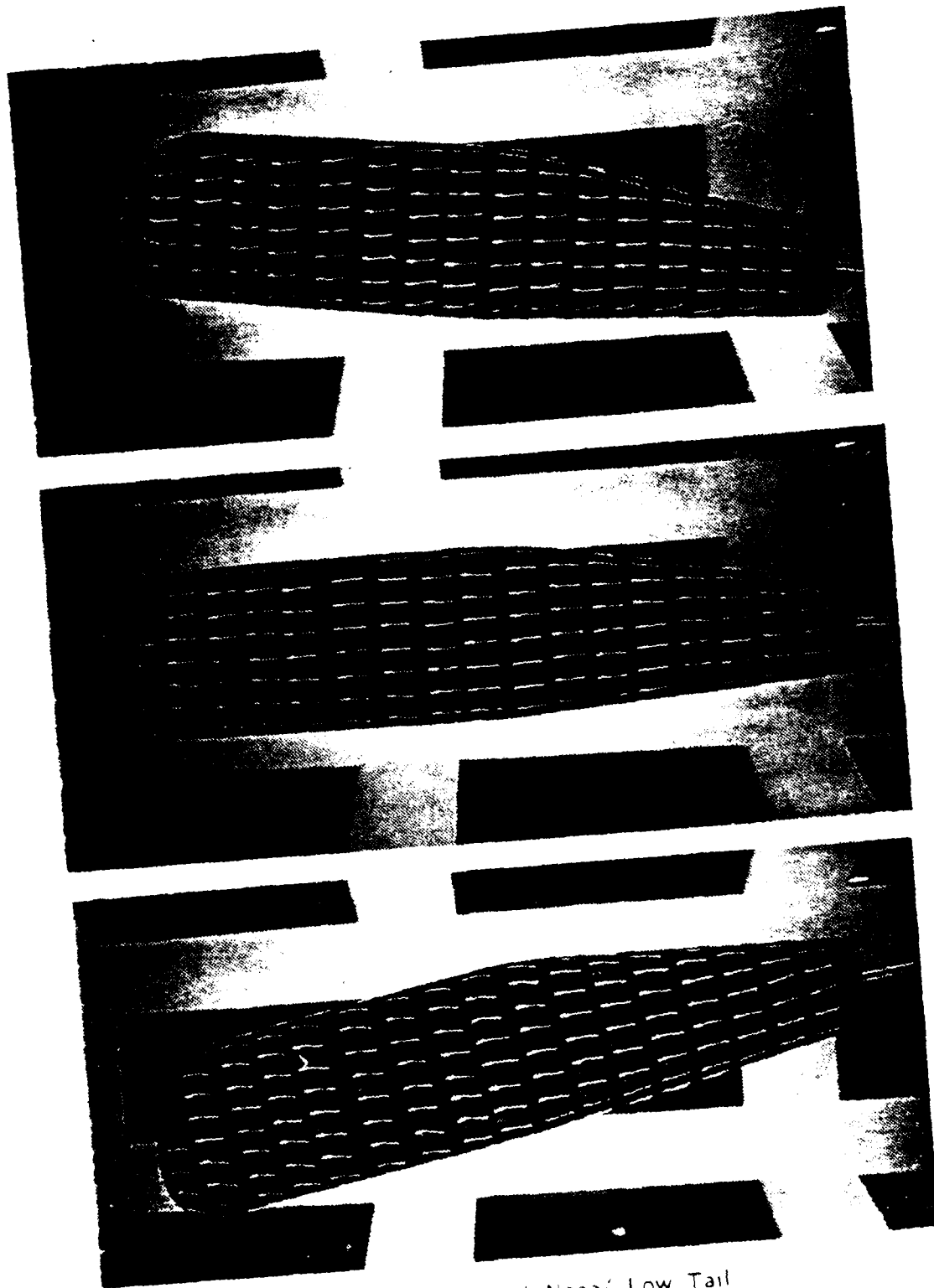


Figure C.6 Blunt Nose/ Low Tail

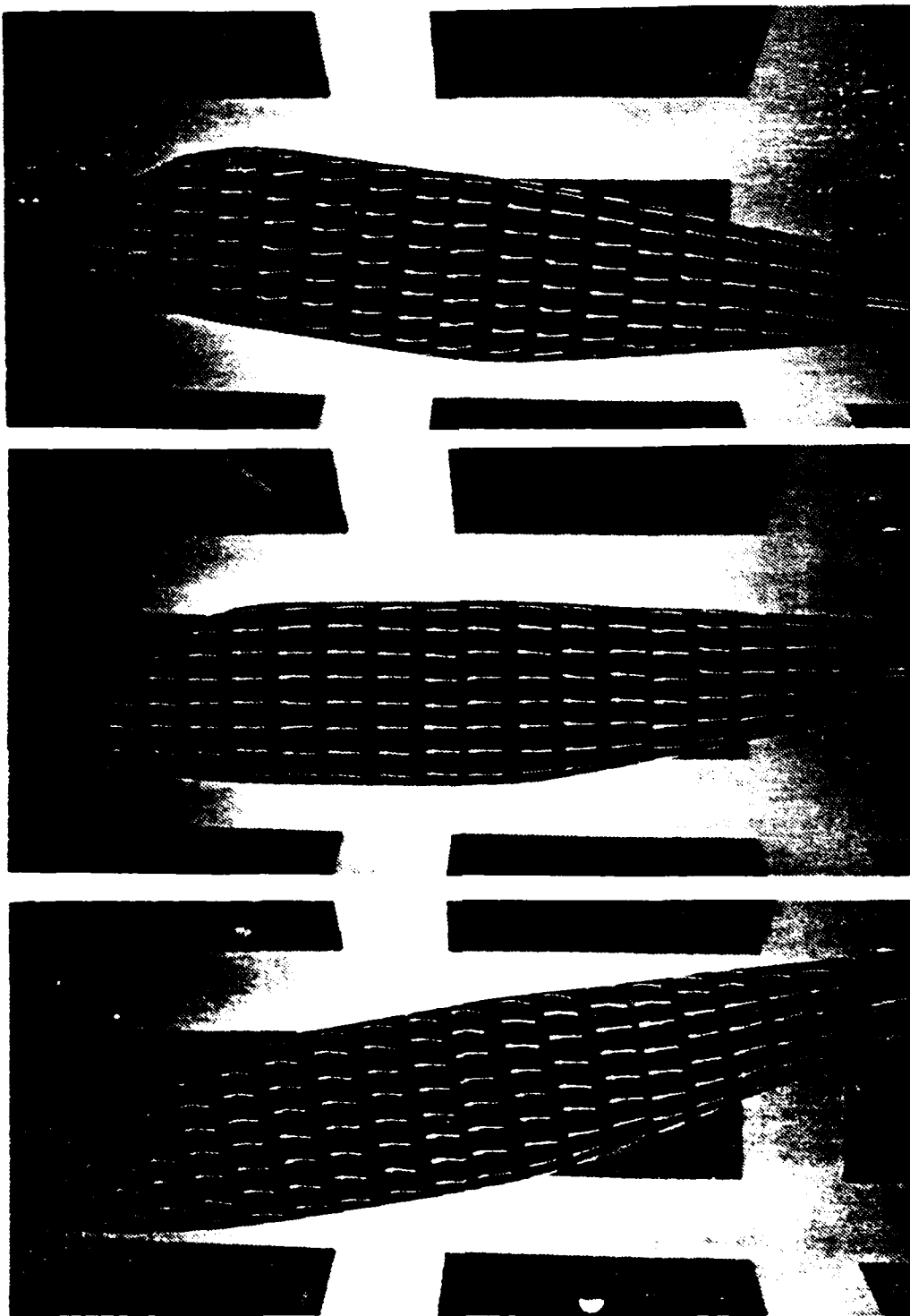


Figure C.7 Smooth Nose/ High Tail

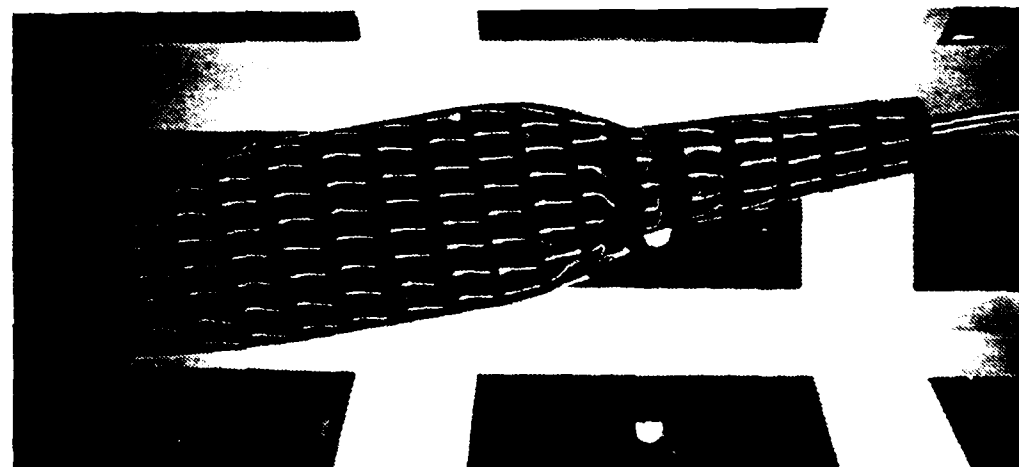
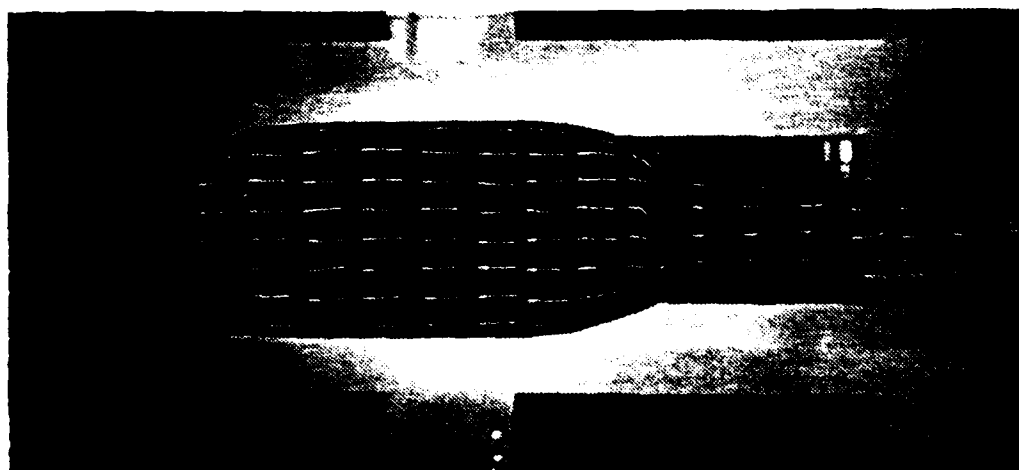
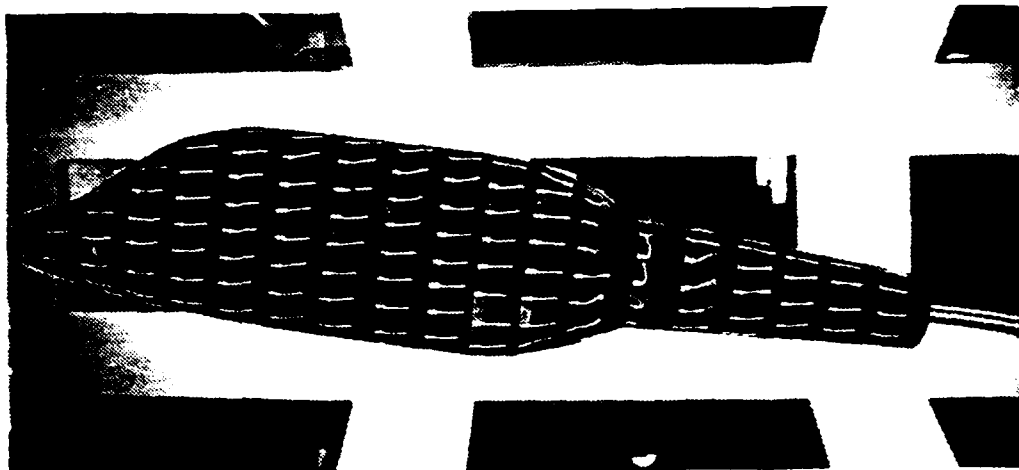


Figure C.8 Smooth Nose/ Symmetric Tail

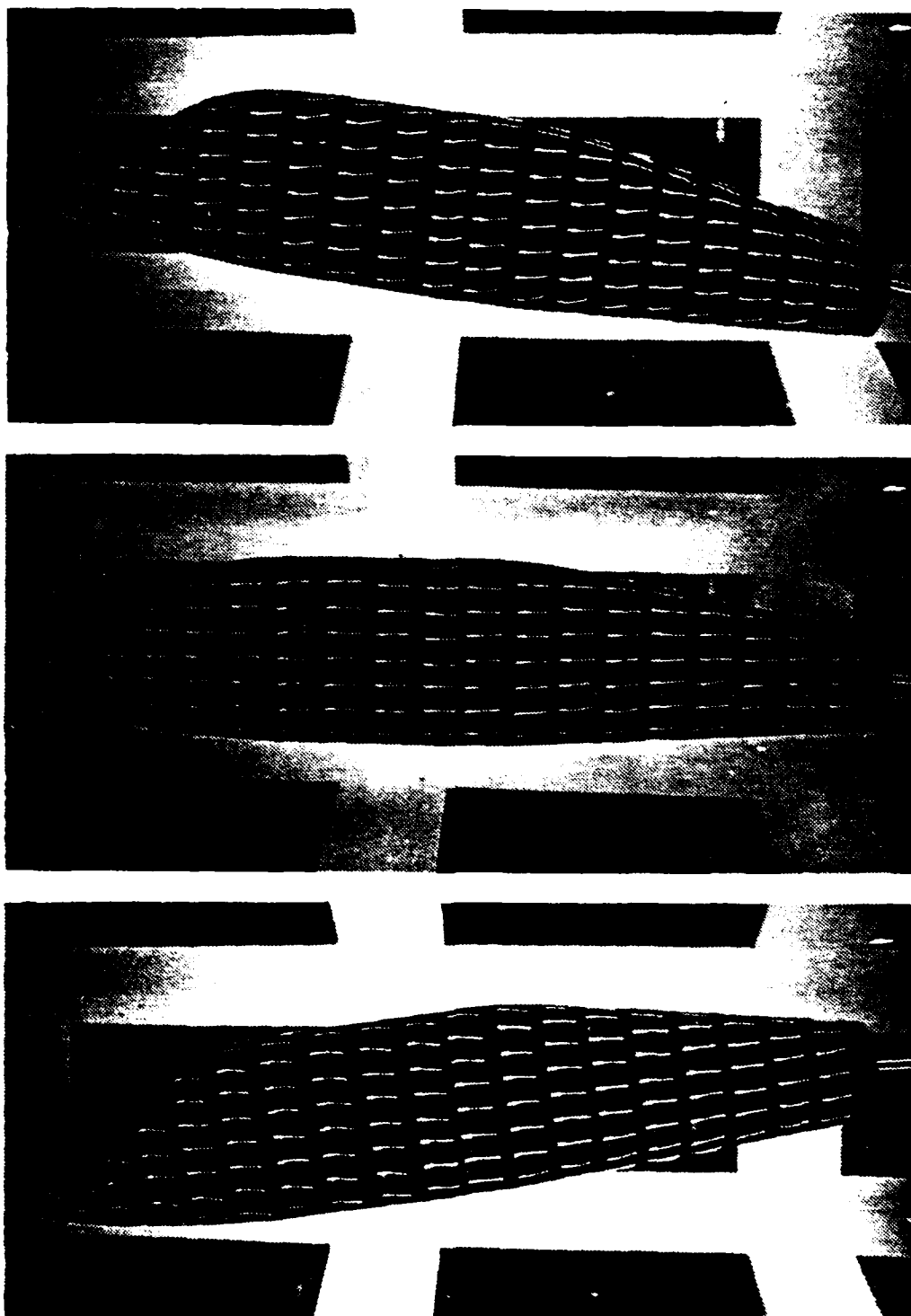


Figure C.9 Smooth Nose/ Low Tail

LIST OF REFERENCES

1. R. Scott Mair, *Wind Tunnel Drag Evaluations of Helicopter Nose Sections*, Naval Postgraduate School Thesis, Monterey, California, 1985.
2. S.M. Gorlin and I.I. Slezinger, *Wind Tunnels and Their Instrumentation*, Israel Program for Scientific Translations, 1966.
3. James P. Crowder, *Add Fluorescent Mini-Tufts to the Aerodynamicist's Bag of Tricks*, *Astronautics and Aeronautics*, Vol. 18, pp. 54-56, Nov 1980.
4. J.P. Holman *Experimental Methods for Engineers*, McGraw-Hill, 1978.
5. Department of Aeronautics, *Laboratory Manual for Low-Speed Wind-Tunnel Testing*, Naval Postgraduate School, Monterey, California, October, 1983.
6. Corning Glass Works, *Color Filter Glasses, Second Edition 1982* Corning, 1982.

BIBLIOGRAPHY

Anderson, John D., Jr., *Fundamentals of Aerodynamics*, McGraw-Hill, 1984

Department of Aeronautics, *Laboratory Manual for Low-Speed Wind-Tunnel Testing*, Naval Postgraduate School, Monterey, California, October, 1983.

Hoerner, Sighard F., *Fluid Dynamic Drag*, Hoerner, 1965

Hoerner, Sighard F., *Fluid Dynamic Lift*, Hoerner, 1971

Jones, Bradley, *Elements of Practical Aerodynamics, Fourth Edition*, Wiley, 1950

Pope, Alan, *Wind-Tunnel Testing*, Wiley, 1947

Robinson, R.F., and Novak, D.H., *Introduction to wind Tunnel Testing, Second Edition*, University Book Store, West Lafayette, Indiana, 1952

INITIAL DISTRIBUTION LIST

	No.	Copies
1. Defense Technical Information Center Cameron Station Alexandria, Virginia 22314	2	
2. Library, Code 0142 Naval Postgraduate School Monterey, California 93943	2	
3. Department Chairman, Code 67 Department of Aeronautics Naval Postgraduate School Monterey, California 93943	1	
4. Prof Donald M. Layton, Code 67-LN Department of Aeronautics Naval Postgraduate School Monterey, California 93943	2	
5. Ted Dunton, Code 67 Department of Aeronautics Naval Postgraduate School Monterey, California 93943	1	
6. Army Aviation Systems Command ATTN: Technical Director 4300 Goodfellow Blvd St. Louis, Missouri 63100	1	
7. Cpt Christopher L. Sargent 2750 Glendower Ave. Los Angeles, California 90027	3	

END

FILMED

8-85

DTIC